5-1-2005

Results of the Fatigue Evaluation and Field Monitoring of the I-39 Northbound Bridge over the Wisconsin River

Robert J. Connor

Hussam N. Mahmoud

Carl A. Bowman

Results of the Fatigue Evaluation and Field Monitoring of the I-39 Northbound Bridge over the Wisconsin River

Final Report

By

Hussam N. Mahmoud
Research Engineer
ATLSS Engineering Research Center

Robert J. Connor
Research Engineer
ATLSS Engineering Research Center

Carl A. Bowman
Instrumentation Technician
ATLSS Engineering Research Center

ATLSS Report No. 05-04

March 2005

ATLSS is a National Center for Engineering Research on Advanced Technology for Large Structural Systems

117 ATLSS Drive
Bethlehem, PA 18015-4729

Phone: (610)758-3525
Fax: (610)758-5902

www.atlss.lehigh.edu
Email: inatl@lehigh.edu

Table of Contents

EXECUTIVE SUMMARY

The I-39 Bridge is located near Wausau, WI and carries, US 51 and I-39 NB over the Wisconsin River. The bridge is a five span continuous steel girder bridge and was opened to traffic in 1961. The bridge crosses the Wisconsin River from the Village of Rothschild on the southeast, to the town of Weston, Marathon County on the Northwest side.

The objective of this study was to assess the serviceability of the bridge by conducting a complete fatigue evaluation of various fatigue prone details and estimate their remaining fatigue life. The overall behavior and the global response of the bridge were also of interest.

The instrumentation consisted of installation of weldable resistance strain gages at key locations both to understand the response of the bridge to load and to quantify the stress-range histograms at critical details. Bondable resistance strain gages were used to measure the out-of-plane bending stresses at the transverse connection plate to web detail. Displacement sensors were also installed at selected locations to measure the out-of-plane displacement of the transverse connection plate and correlate between the measured displacement and stresses. Controlled load tests using test trucks of known weight and geometry were conducted. In addition, long-term monitoring of random traffic was performed.

The remaining fatigue life of the instrumented details was estimated using stress-range histograms determined from the long-term monitoring data. Retrofit solutions were recommended for locations where the estimated remaining life was 50 years or less. The recommended retrofits include:

- Hammer peening technique to improve the fatigue strength of cover plate details at girder field splices.
- Increasing the fatigue strength at the lateral shelf plate details was recommended by bolting an additional plate to the bottom flange of the girders at selected locations.

1.0 Introduction

1.1 Bridge Description

Built in 1961 in Wausau, Wisconsin, Bridge B-37-75 is a five span continuous steel plate girder bridge, which carries the northbound traffic of Interstate 39 and US 51over the Wisconsin River. The girders are slightly kinked at field splices to accommodate a horizontal curve. The bridge is symmetrical about the mid point of the 3rd span and has a total length of 643'-2 3/8". The length of the first, second, and third spans are 109'-7 1/4", 139'-10 3/4", and 140'-0", respectively. Figure 1.1 shows both north and south bound bridges over the Wisconsin River looking northwest.

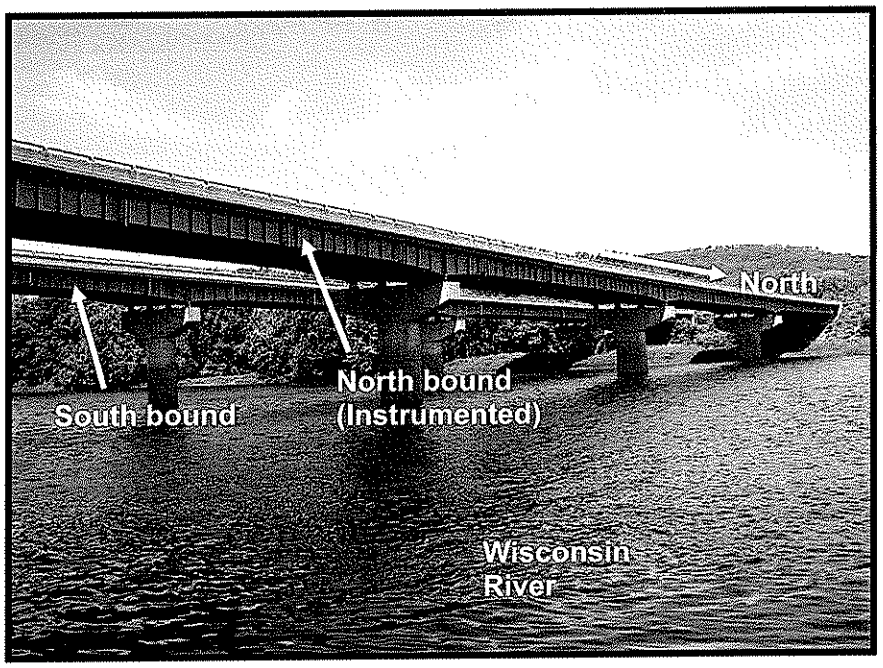

Figure 1.1 – Elevation view of the north bound and the south bound bridges over the Wisconsin River

The objective of this study was to assess the serviceability of the bridge by conducting a complete fatigue evaluation of various fatigue prone details on the bridge and estimate their remaining fatigue life. This was done through long-term monitoring, which was conducted to measure the stress ranges at critical details. The data was then utilized to estimate the remaining fatigue life of the detail in question.

Also of interest were the overall behavior and global response of the bridge to live loads. To capture data necessary to allow researchers to understand the bridge's overall behavior and response, strain gages and displacement sensors were installed in various locations on the bridge girders. The location of the sensors was selected to capture the maximum response of the bridge girders to moving loads as well as the load distribution between all girders.

All field work was conducted over the period between July and November 2004 by personnel from at the ATLSS Center at Lehigh University, Bethlehem, PA.

2.0 Instrumentation Plan and Data Acquisition

The same instrumentation plan was used for both the controlled truck load testing and the long-term monitoring as described in the following section. Instrumentation was installed in the first two spans on the bridge. A line girder analysis was used to roughly estimate the location where the stresses would be the maximum. A detailed description of the location of the strain gages and the Linear variable differential transformers (LVDT's) instrumented on the spans can be found in Appendix A.

2.1 Strain Gages

Strain gages were installed to understand the local response of particular details and to establish the global response of the bridge as a system. Both weldable and bondable uniaxial strain gages were used. In most locations weldable gages were used since they are much easier to install in the field than bondable gages. The weldable gages were type LWK-06-W250B-350, with an active grid length of 0.25 inches. The weldable gages were pre-bonded to a metal strip by the manufacturer and spot welded to the tested structure in the field.

The bondable gages were type EA-06-125BZ-350 with an active grid length of 0.125 inches. The gages were attached to the steel using a special adhesive at the desired location.

The metal surfaces were ground and cleaned before installing the weldable and the bondable gages. After installation, gages were covered with multi-layer system then sealed with silicon type agent.

Both types of gages were produced by Measurements Group Inc and are temperature-compensated for use on structural steel. The gages resistance is 350Ω and an excitation voltage of ten volts was used.

2.2 Displacement Sensors

Linear variable differential transformers (LVDTs) were mounted to magnetic bases installed on the bridge. The sensors, manufactured by Macro Sensors, have a displacement range of 1/4 inch with infinite resolution. The resolution of the measurement is limited by the data acquisition system. As configured during this study, the resulting resolution was better than 0.01 mils. The sensors are encased in stainless steel housings and are suitable for use in harsh environments.

2.3 Data Acquisition

A Campbell Scientific CR9000 Data Logger was used for the collection of the data throughout the controlled testing and long-term monitoring. The logger is a high-speed, multi-channel, 16-bit system configured with digital and analog filters to assure noise-free signals. By connecting a laptop computer to the logger, real-time data were viewed to assure that all sensors were functioning properly and review the response of the bridge during testing. Figure 2.2 shows the data acquisition system used including the LVDT's power supply and a power conditioner. The data logger, the LVDT's power supply, and the power conditioner were enclosed in a weather-tight steel box as shown in Figure 2.3 located on the abutment.

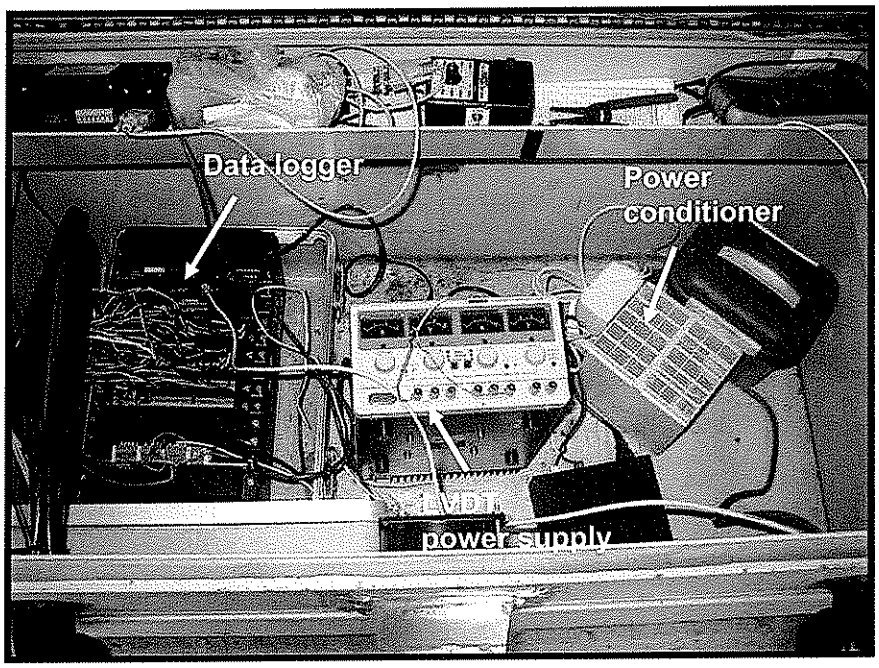

Figure 2.2 – Data acquisition system

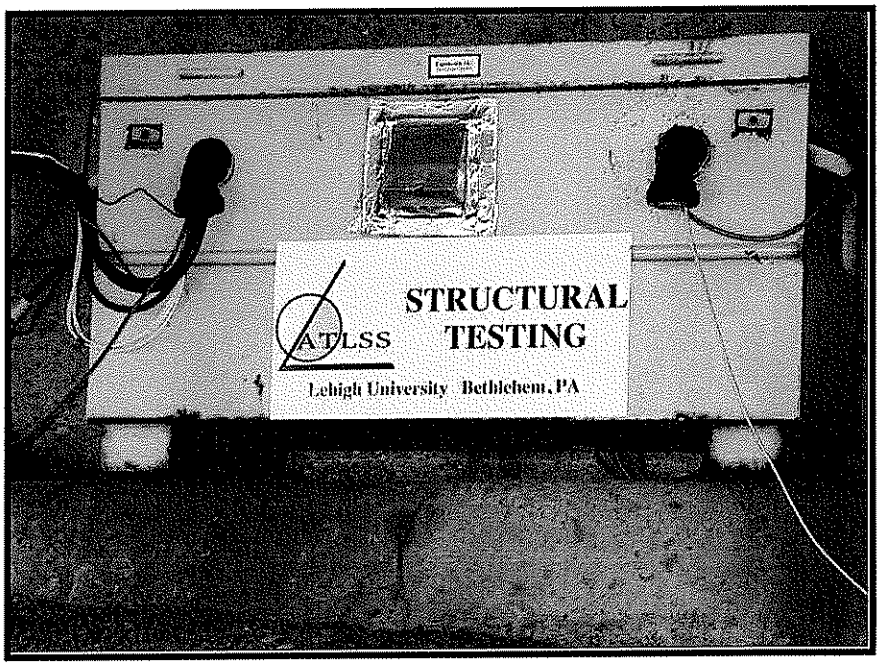

Figure 2.3 – Weather-tight enclosure containing data acquisition system

2.4 Remote Long-term Monitoring

The CR9000 data logger remained in place and was also used for long-term monitoring of the bridge. During the remote monitoring phase, both time history data and stress-range histograms were recorded.

To minimize the volume of data collected during recording of the stress-time-history files, data were not recorded continuously. A predefined lower limit stress value (i.e., trigger), for two gages was used to control when recording of the data began and ended. Once the strain value for that gage reached the predefined limit, the logger began recording data for all sensors on the bridge. Gages used to trigger the recording of data were selected so that northbound traffic in each lane could be identified and stored in separate files.

Stress-range histograms were developed at selected locations. These locations were selected based on the results of the controlled load tests and monitoring of random traffic while on site. The stress range histograms were divided into 0.5 ksi bins and cycles less than 0.2 ksi were not counted. The histograms were not dependent on triggers. Hence, all cycles were counted.

Approximately after a month of consistent monitoring of the bridge, a decision was made to install a video camera on the bridge. The camera was mounted on the bridge and was triggered to record data by the logger for a predefined period of time when a moving vehicle caused the strain to reach a certain defined value in a particular channel. The video data recorded by the camera provided valuable information on the identification of the configuration, position, and number of trucks producing a specific large stress cycle on the bridge.

Remote communication with the logger and camera was established using a wireless cellular modem. The remote communication allowed program upload and data download to be performed from the ATLSS Research Center in Bethlehem, PA.

3.0 Controlled Load Testing

A series of controlled load tests were conducted using two test trucks. The first truck, with ID number 169 (heavier truck), had three main axles and two floating axles. The second truck, with ID number 160 (lighter truck), had three main axles and one floating axle. Tests were conducted with both trucks having their floating axles in the "up" position. Both test trucks were fully loaded with gravel. The gross vehicle weight (GVW) of the heavier truck and the lighter truck was 74,620 pounds and 67,200 pounds, respectively. Figure 3.1 shows the heavy truck, while Figure 3.2 shows the lighter truck. The geometry and the axle load data of the heavier truck are listed in Table 3.1 and Table 3.2, respectively. Similarly, the geometry and the axle load data of the lighter truck are listed in Table 3.3 and Table 3.4, respectively.

Figure 3.1 – Test truck # 169 (heavier truck) used in the controlled load testing

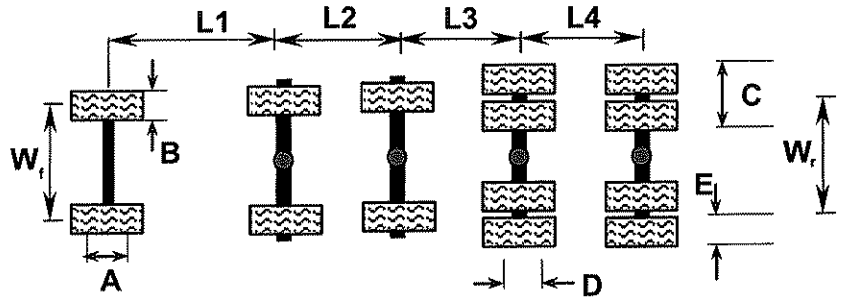

Rear Axle	L1 (in)	L2 (in)	L3 (in)	L4 (in)	W_f (in)	W_r (in)	A[1] (in)	B (in)	C (in)	D[1] (in)	E (in)
Tandem	98	47.5	51.5	53.5	84	71	-	13	21.75	-	10.5

Note:
1. Parameter not measured

Table 3.1 – Geometry of test truck #169 (heavier truck) used in the controlled load tests

Test Description	Rear Axle Type	Front Axle Load (lb)	Rear Axle Group Load (lb)	GVW[1] (lb)	Date of Tests
Controlled Load Tests	Triaxle	15,220	59,400	74,620	July 28, 2004

Note:
1. GVW = Gross Vehicle Weight

Table 3.2 – Axle load data of test truck # 169 (heavier truck)

Figure 3-2 – Test truck # 160 (lighter truck) used in the controlled load testing

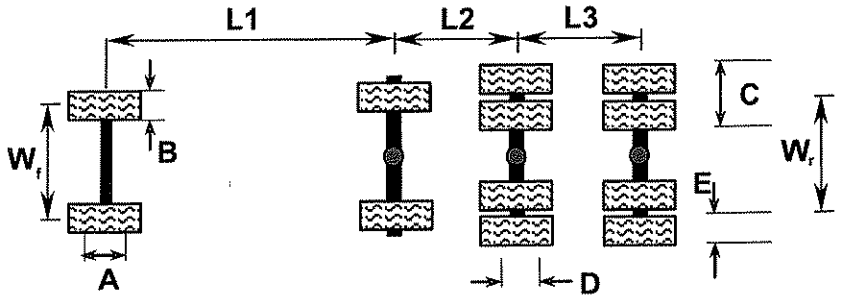

Rear Axle	L1 (in)	L2 (in)	L3 (in)	W_f (in)	W_r (in)	A[1] (in)	B (in)	C (in)	D[1] (in)	E (in)
Tandem	103	75	52	83	71	-	10.50	22.50	-	10.50

Note:
1. Parameter not measured

Table 3.3 – Geometry of Test truck #160 (lighter truck) used for the controlled load tests

Test Description	Rear Axle Type	Front Axle Load (lb)	Rear Axle Group Load (lb)	GVW[1] (lb)	Date of Tests
Controlled Load Tests	Triaxle	26,280	40,920	67,200	July 28, 2004

Note:
1. GVW = Gross Vehicle Weight

Table 3.4 – Axle load data for test truck # 160 (lighter truck)

The controlled load tests were conducted on July 28, 2004 between 9 AM and 11 AM. To eliminate any disruption that could be caused by other traffic passing over the bridge while testing, traffic on the northbound of I-39 was stopped by Wisconsin State Patrol (approximately 2 miles south of the bridge). An on ramp just south of the bridge was also closed by WisDOT personal during testing to prevent any vehicles from crossing the bridge at the time of testing.

The tests consisted of a series of seven crawl and four dynamic tests. In all tests the trucks traveled northbound. The crawl tests started at the south abutment and the test truck(s) was driven at approximately 5 miles per hour across the bridge. The dynamic tests were conducted with the truck traveling at speeds of approximately 45 mph in the first test and 65 mph in the remaining three tests. To achieve the desired speed in the dynamic tests, traffic was controlled by the State Patrol approximately one mile south of the test truck (2 miles south of the bridge) to allow enough distance for the test truck to achieve the required speed.

Testing was conducted across the bridge in either the inside right lane, the outside left lane, or in both lanes (side-by-side). A total of seven crawl tests were conducted. The first two tests were conducted with the heavier test truck traveling in the right lane at a speed of 5 miles per hour. In the third and fourth tests, the heavier truck was also used with a speed of 5 miles per hour traveling in the left lane. In the fifth and sixth tests, both the heavier and the lighter test trucks were traveling side-by-side at speed of 5miles per hour, where the heavier truck was in the right lane and the lighter truck was in the left lane. In the seventh crawl test, both trucks were traveling back-to-back in the right lane at 5 miles per hour speed with the heavier truck ahead of the lighter truck.

A total of four dynamic tests were conducted. The heavier test truck was used in all four tests. The first two tests were conducted in the right lane with the truck traveling at a speed of 45 mph and 65 mph, respectively. In the third and the fourth tests, the truck was traveling in the left lane at a speed of 65 mph.

3.1 Controlled Load Tests

A summary of the controlled load tests data are presented in Tables 3.1

Test	Speed (mph)	Direction	Truck Number	Location
CNBRT_1.Dat	5	NB	Heavier	Right lane
CNBRT_2.Dat	5	NB	Heavier	Right lane
CNBLT_1.Dat	5	NB	Heavier	Left lane
CNBLT_2.Dat	5	NB	Heavier	Left lane
CSBS_1.Dat	5	NB	Heavier truck in inner lane and lighter truck in outer lane	Both lanes (side-by-side)
CSBS_2.Dat	5	NB	Heavier truck in inner lane and lighter truck in outer lane	Both lanes (side-by-side)
CTT_1.DAT	5	NB	Back-to-back, heavier truck ahead of lighter truck	Right Lane
DNBRT_1.DAT	45	NB	Heavier	Right lane
DNBRT_2.DAT	65	NB	Heavier	Right lane
DNBLT_1.DAT	65	NB	Heavier	Left lane
DNBLT_2.DAT	65	NB	Heavier	Left lane

Table 3.1 – Summary of the controlled load tests

4.0 Summary of Instrumentation Layout

The following section summarizes the instrumentation plan used on the bridge. Detailed instrumentation plans are included in Appendix A.

4.1 Strain Gages on Main Girders

A total of 24 strain gages were installed on the flanges and the webs of the main girders at various fatigue prone details to assess the remaining service life of the bridge. The details on the bridge, which are susceptible to fatigue cracking include welded full penetration flange splices, welded flange cover plates at field splices, lateral shelf plate connections welded to bottom flanges, and welded transverse stiffeners to webs of main girders. The locations where the gages were installed were also chosen such that the overall behavior and global response of the bridge could be examined.

4.1.1 Welded Full Penetration Flange Splice

In all four girders (G1 through G4) flange plates are spliced together using full penetration welds. Where plates of different thickness were spliced, weld reinforcement was not ground smooth and the details are therefore classified as category C. Four strain gages, CH_11, CH_12, CH_13 and CH_14, were installed in the longitudinal direction on the bottom faces of the bottom flanges. The gages were installed in span 1, between P.P. 5 and P.P. 6 on girders G4 through G1, respectively. The gages were installed 3 inches away from the weld toe to measure the magnitude of the nominal stress range at the details as shown in Figure 4.1.

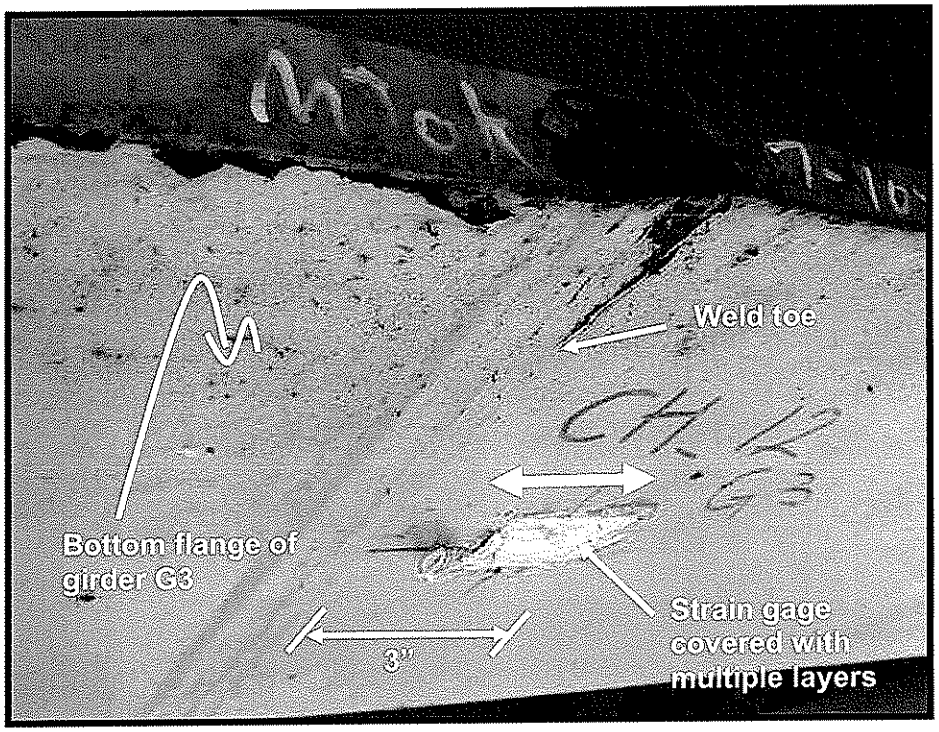

Figure 4.1 – CH_12 installed in span 1 between P.P. 5 and P.P. 6 on the bottom face of the bottom flange of girder G3 (3 inches away from weld toe)

4.1.2 Cover Plate at Field Splice

Cover plates were used as fill plates and were welded to the bottom face of the bottom thinner flange to account for the difference in the thickness between the two spliced flanges. As shown in Figure 4.2, strain gages were installed, 3 inches away from the weld (toe) used for attaching the cover plates to the bottom flanges, to measure the nominal stress range and assess the remaining fatigue life of the detail. A total of six channels were installed at two different cross sections. At the first cross section, CH_3 through CH_6 were installed in span 1 at P.P. 5 on girders G4 through G1, respectively. At the second cross section, CH_15 and CH_16 were installed in span 2 at P.P. 9 on girder G4 and girder G3, respectively.

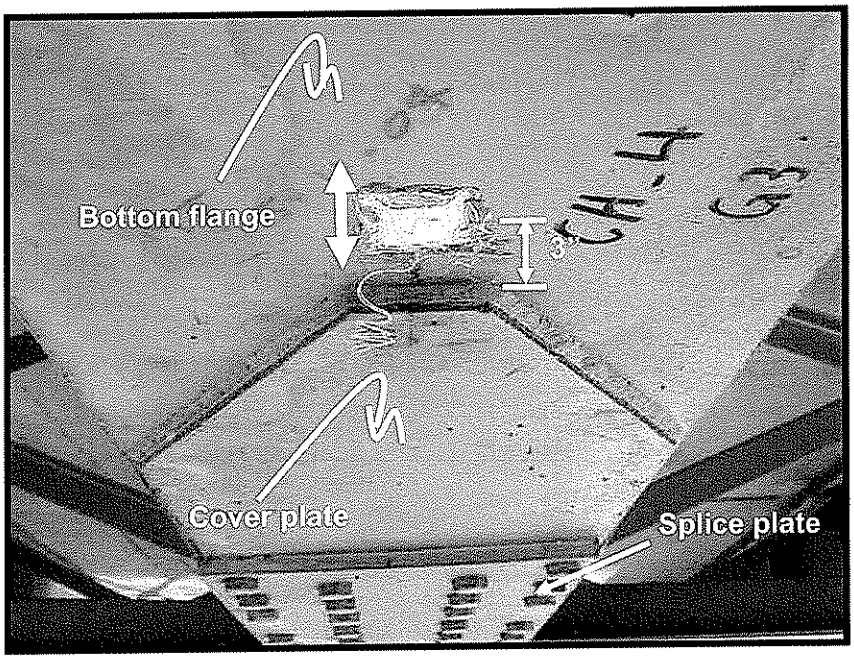

Figure 4.2 – CH_4 installed in span 2 at P.P. 9 on the bottom face of the bottom flange of girder G3 (3 inches away from weld toe)

4.1.3 Lateral Shelf Plate Connection to Bottom Flange

Lateral shelf plates were welded to the top face of the bottom flange in order to connect the lower horizontal strut of the diaphragm and lower wind bracing members to the main girders. In some cases, depending on the location of the shelf plates on the bridge, the shelf plates were welded to the bottom flanges all around the shelf plate. In other locations only longitudinal welds were used to attach the shelf plates to the bottom flanges. Where the plate was not welded all around, accumulation of corrosion product between the shelf plate and the bottom flange can be produced and potentially cause pack-out failure of the welds.

The nominal stress range at the detail was monitored by installing six strain gages on the top faces of the flanges of the main girders 3 inches away from the edge of the lateral plate (Figure 4.3). The channels were installed at two different cross sections.

Four channels were installed on the four girders at the first cross section. Specifically, CH_17 through CH_20 were installed in span 2 at P.P. 13 on girders G4 through G1, respectively. The remaining two channels (CH_1 and CH_2) were installed in span 1 at P.P. 3 on girders G4 and G3, respectively.

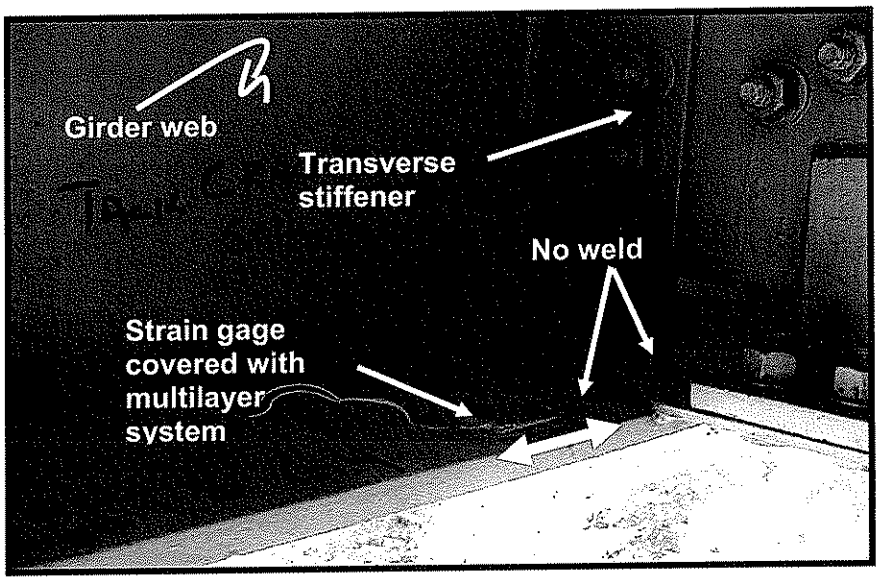

Figure 4.3 – CH_1 installed on the top face of the bottom flange of girder G4 in span 1 at P.P. 3

4.1.4 Transverse Connection Plate to Web Detail

Out-of-plane distortion cracks are known to develop when relative displacement occurs between the transverse connection plate and flange. The displacement occurs only at locations where the transverse connection plates are not welded to the flange. On the I-39 bridge, the transverse connection plates were not welded to flanges subjected to live load tensile stresses.

In order to evaluate the potential for cracking, eight bondable strain gages were installed at four different connections where the potential for cracking existed to measure the stresses caused by the relative displacement (if any). At every location, two gages were installed on the web of a specified girder. One gage was installed adjacent to the toe of the vertical weld used for connecting the transverse connection plate to the web of the girder (Figure 4.4) and the other gage was installed on the opposite face of the web, directly behind the other gage (i.e. CH_7 was installed behind CH_8, CH_10 was installed behind CH_9, CH_22 was installed behind CH_21, and CH_24 was installed behind CH_23).

CH_7, CH_8, CH_9, and CH_10 were installed in span 1 at P.P. 5. CH_7 and CH_8 were installed on the web of girder G4, while CH_9 and CH_10 were installed on the web of girder G3. Similarly, CH_21, CH_22, CH_23, and CH_24 in span 2 at P.P. 13 where CH_21 and CH_22 were installed on the web of girder G4, and CH_23 and CH_24 were installed on the web of girder G3.

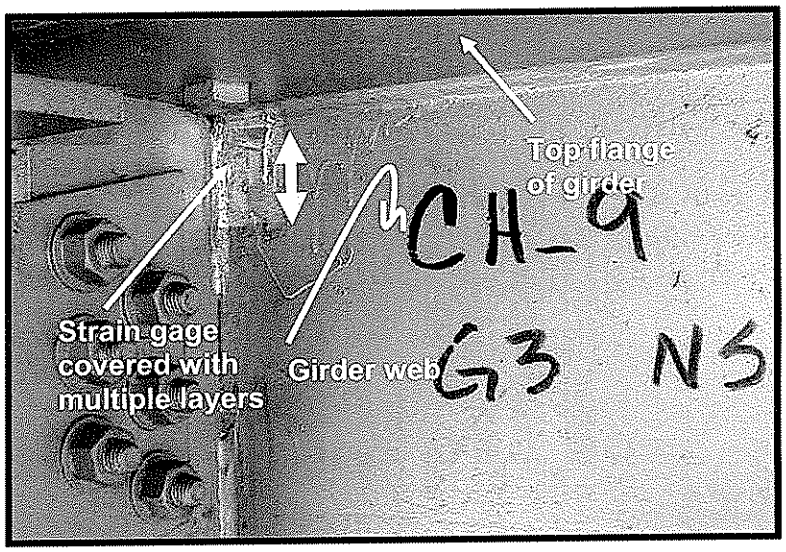

Figure 4.4 – CH_9 installed in span 1 at P.P. 5 on the web of girder G3 adjacent to the weld toe of the transverse connection plate.
Channel CH_10 is directly behind CH_9 on the opposite face of the web

4.2 Displacement Sensors

Two Linear Variable Differential Transformers (LVDT's) were placed to correlate between the stresses measured and the relative displacement between the transverse connection plates and the web of the girders. CH_25 was installed on girder G4 in span 1 at P.P. 5, while CH_26 was installed on girder G3 in span 2 at P.P. 13. A typical installation of the LVDT on girder G4 in span 1 at P.P. 5 is shown in Figure 4.5.

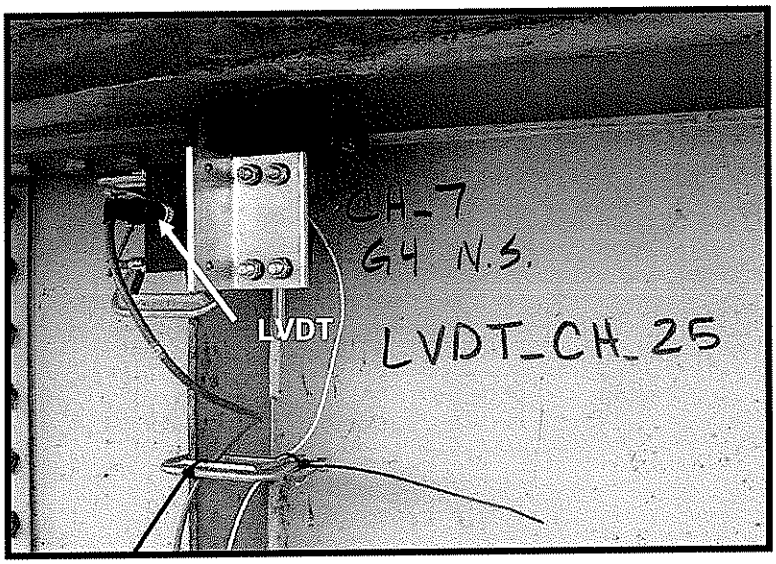

Figure 4.5 – LVDT (CH_25) installed on the web of girder G4 in span 1 at P.P. 5 to measure out-of-plane displacement

5.0 Results of Controlled Load Tests

The results of the controlled static and dynamic load tests are discussed in this section.

5.1 General Response

In general, the response of the bridge was as expected and typical of a continuous multi-span bridge. Figure 5.1 presents the response of CH_3, CH_4, CH_5 and CH_6 as the test truck passed over the right lane in test CNBRT_2. Channels CH_3, CH_4, CH_5 and CH_6 were installed in span 1 at P.P. 5 on the bottom flanges of girders G4 through G1, respectively. As expected, the response in all four channels is positive and maximum as the test truck passed over the first span (where the channels were installed) and becomes negative and less in absolute magnitude as it passes into the second span and subsequent spans.

The figure also shows good load distribution between the girders. The maximum response in the instrumented girders was observed when the test truck was directly located over the detail and lower response was observed in the girders further away from the test truck. This is evident as the test truck passed over span 1 and span 2. The observation becomes less clear as the test truck passed over span 3 and diminishes as the truck passes over span 4 and span 5. This is a typical behavior expected in a continuous bridge due to the substantial transverse and longitudinal load distribution which occurs as loads move further away from the instrumented section.

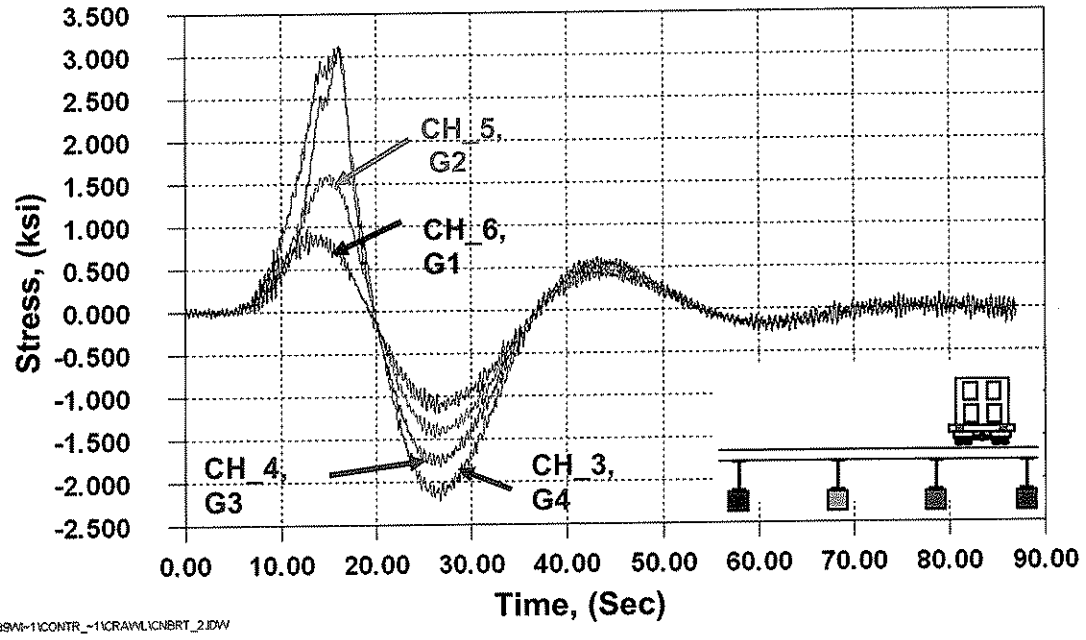

Figure 5.1 – Response of CH_3 through CH_6 installed in span 1 at P.P. 5 on girders G4 through G1 respectively (on the bottom flanges at the end of the cover plates) as the heavier test truck passed over the right lane in the crawl test (CNBRT_2) (View looking north)

Figure 5.2 shows an evenly shared load by all girders as both test trucks passed side-by-side over the bridge. The small change in the magnitude of stress in the channels could be attributed to the slight difference in the weight between both test trucks and normal test variability. It was also observed that unlike the response shown in Figure 5.1, the first response of the channels at this cross section as the truck passes directly over them in the first span is negative and not maximum as expected. The observation confirms the fact that CH_11 through CH_14 were instrumented in the negative moment region slightly past the inflection point.

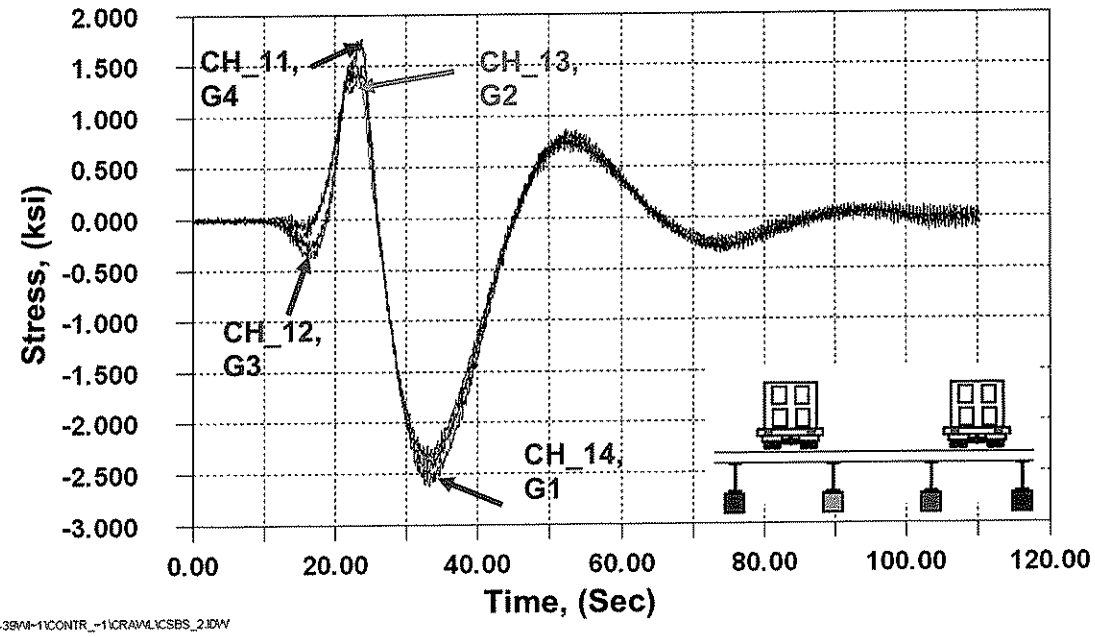

Figure 5.2 – Response of CH_11 through CH_14 installed in span 1 between P.P. 5 and P.P. 6 on girders G4 through G1 respectively (on the bottom flanges at flange splices) as both test trucks passed side-by-side over the bridge in the crawl test (CSBS_2) (View looking north)

Figure 5.3 shows that unlike CH_11 and CH_12, the first response in CH_13 and CH_14 is positive when the test truck passed over the right lane. This is an indication of that composite action between the girders and the slab as girders G2 and G1 (further away from the load) are being lifted up with the slab. The response is due to torsional deformation as the load is applied eccentrically on the deck and is common in bridges of this configuration. For such torsional effects to be transferred transversely, the slab and the steel cross frames participate in spreading the load. The entire span can be idealized as a stiffened plate. That is, the slab acts as a plate while the girders can be thought of as deep stiffeners. As expected, this behavior is reversed when the test truck passed in the left lane. As indicated in the figure, the test trucks took approximately 90 seconds to cross the bridge spans (639.2 ft). The average speed is therefore, 7.1ft/sec or 4.8miles/hr.

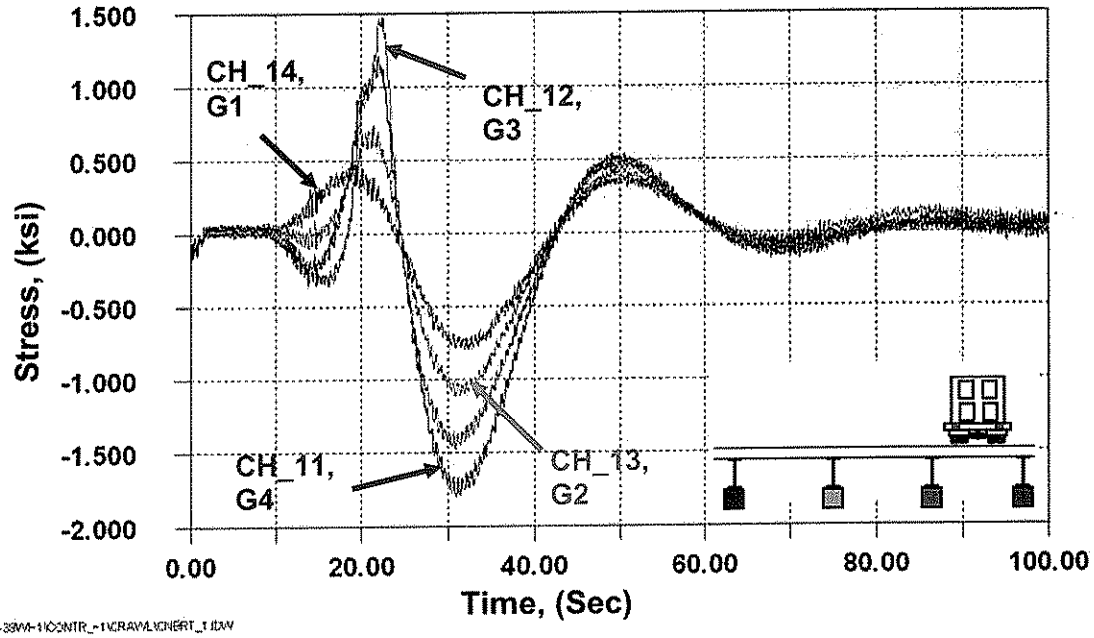

Figure 5.3 – Response of CH_11 through CH_14 installed in span 1 between P.P. 5 and P.P. 6 on girders G4 through G1 respectively (on the bottom flanges at flange splices) as the test truck passed over the bridge in the right lane in the crawl test (CNBRT_1) (View looking north)

5.2 Repeatability of Data

Except for the crawl back-to-back test, all crawl tests were repeated. The dynamic tests were also repeated. However, for the first two dynamic tests performed in the right lane (DNBRT_1 and DNBRT_2), the test truck passed over the bridge with a speed of 45 mph in the first dynamic test and 65 mph in the second dynamic test. Data obtained show consistency between the repeated tests. Similar behavior between the crawl and the dynamic tests was observed with dynamic amplification factor of approximately 1.05.

5.3 Stresses in Girder Flanges at Welded Full Penetration Flange Splice

As mentioned previously, gages were installed in the longitudinal direction on the bottom face of the flanges of the main girders to measure the nominal bending stress near the welded full penetration flange splice. This detail is classified as category C detail with constant amplitude fatigue limit (CAFL) of 10 ksi. To measure the nominal stresses near the details, CH_11 through CH_14 were installed in span one between P.P. 5 and P.P. 6 on girders G1 through G4, respectively. Figure 5.3 presents a typical response of the instrumented detail to a moving load. A summary of the maximum stress, minimum stress, and stress range values experienced by the channels in the crawl tests is presented in Table 5.1.

Span 1, Between P.P. 5 and P.P. 6						
Truck in lane	Bottom flange (ksi) (CH_11, G4)			Bottom flange (ksi) (CH_12, G3)		
	σ_{max}	σ_{min}	$\Delta\sigma$	σ_{max}	σ_{min}	$\Delta\sigma$
Right	1.2	-1.7	2.9	1.4	-1.4	2.9
Left	0.3	-0.7	1.0	0.5	-1.1	1.6
Side-by-side	1.5	-2.3	3.9	1.8	-2.3	4.1
Train (right lane)	1.3	-3.0	4.3	1.3	-2.4	3.7

Span 1, Between P.P. 5 and P.P. 6						
Truck in lane	Bottom flange (ksi) (CH_13, G2)			Bottom flange (ksi) (CH_14, G1)		
	σ_{max}	σ_{min}	$\Delta\sigma$	σ_{max}	σ_{min}	$\Delta\sigma$
Right	0.6	-1.1	1.7	0.4	-0.7	1.2
Left	1.3	-1.5	2.8	1.1	-1.9	3.0
Side-by-side	1.6	-2.4	4.0	1.5	-2.6	4.0
Train (right lane)	0.7	-1.8	2.6	0.6	-1.3	1.9

Table 5.1 – Summary of peak measured bending stresses, in the bottom girder flanges at the welded full penetration flange splice for the various test truck lane positions in the crawl tests

5.4 Stresses in Girder Flanges near Welded Shelf Plate Details

Shelf plates welded to the top face of the bottom flanges exist in many locations on the bridge. The detail is classified as category E detail with CAFL of 4.5 ksi. Six channels (CH_1, CH_2, and CH_17 through CH_20) were installed to monitor the response to live load imposed by the test trucks in the crawl and dynamic tests. Channels CH_1 and CH_2 were installed in span one at P.P. 3 on girders G4 and G3 respectively, while CH_17 through CH_20 were installed in span 2 at P.P. 13 on girders G4 through G1, respectively. Figure 5.4 shows the response of CH_17 through CH_20, with maximum response at CH_17. It is noted that the response at CH_17 is higher than that of CH_18. This is because CH_17 was installed on G4, an exterior girder. Since there is no girder to the right of G4, it cannot shed any load to the right. The load is shed from girder G3 (CH_18) to G4 (CH_17) and G2 (CH_19). Hence, the stresses are lower at CH_18. This response is different than observed from the measurements presented in Figure 5.1, but are not surprising or of concern. It is also worth noting that as the figure shows, the magnitude of the stress (negative) in CH_18 and CH_19 is the same as the test truck passes over the third span in the bridge. This observation is consistent in all crawl tests performed. As discussed, the bridge behaves more as a unit at a given section when subjected to loads applied some distance away. Table 5.2 lists the magnitude of the maximum stress, the minimum stress and the stress range of CH_1, CH_2 and CH_17 through CH_20 in the different crawl tests.

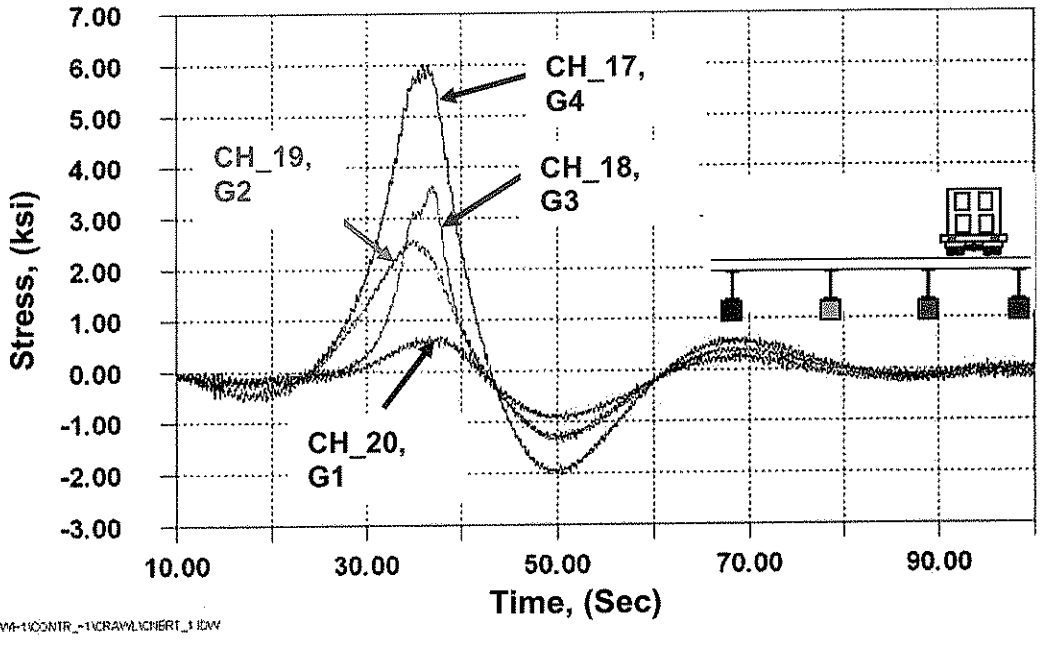

Figure 5.4 – Response of CH_17 through CH_20 installed in span 2 at P.P. 12 on girders G4 through G1 respectively (on the top face of the bottom flanges near welded shelf plates) as the test truck passed over the bridge in the right lane in the crawl test (CNBRT_1)
(View looking north)

Span 1, P.P. 2						
Truck in lane	Bottom flange (ksi) (CH_1, G4)			Bottom flange (ksi) (CH_2, G3)		
	σ_{max}	σ_{min}	$\Delta\sigma$	σ_{max}	σ_{min}	$\Delta\sigma$
Right	5.6	-1.1	6.7	4.4	-1.0	5.4
Left	1.9	-0.7	2.6	0.7	-0.8	1.5
Side-by-side	6.3	-1.7	8.0	6.0	-1.7	7.7
Train (right lane)	7.7	-2.0	9.7	5.2	-2.0	7.2

Span 2, P.P. 13						
Truck in lane	Bottom flange (ksi) (CH_17, G4)			Bottom flange (ksi) (CH_18, G3)		
	σ_{max}	σ_{min}	$\Delta\sigma$	σ_{max}	σ_{min}	$\Delta\sigma$
Right	5.9	-2.0	7.9	3.6	-1.3	4.9
Left	0.9	-0.8	1.4	2.5	-1.0	3.6
Side-by-side	6.1	-2.6	8.7	5.5	-2.2	7.7
Train (right lane)	8.9	3.6	12.5	4.5	-2.2	6.7

Span 2, P.P. 13						
Truck in lane	Bottom flange (ksi) (CH_19, G2)			Bottom flange (ksi) (CH_20, G1)		
	σ_{max}	σ_{min}	$\Delta\sigma$	σ_{max}	σ_{min}	$\Delta\sigma$
Right	2.5	-1.3	3.8	0.6	-0.9	1.5
Left	4.0	-1.4	5.4	5.5	-1.8	7.3
Side-by-side	5.9	-2.6	8.5	6.1	-2.6	8.7
Train (right lane)	4.6	-2.2	6.8	0.9	-1.4	2.3

Table 5.2 – Summary of peak measured bending stresses in the bottom girder flanges near welded shelf plates for the various test truck lane positions in the crawl tests

5.5 Stresses in Girder Flanges near Cover Plates

Cover plates were used as fill plates in locations where two different flange thicknesses are spliced together. Cover plates are known to be fatigue prone details in which cracks could initiate at the termination of the weld used for attaching the cover plates to the flanges. The detail is classified as category E detail per AASHTO specifications with a CAFL of 4.5 ksi. Six channels were installed at different locations to measure the nominal stress near the cover plate detail. Channels CH_3 through CH_6 were installed in span 1 at P.P. 5 on girders G4 through G1, respectively. Channels CH_15 and CH_16 were installed in span 2 at P.P. 9 on girders G4 and G3, respectively.

Figure 5.5 shows the response of CH_3 through CH_6 installed as the heavier test truck passed over the right lane in the crawl test (CNBRT_1). As illustrated in the figure, high stress ranges were recorded in CH_3 and CH_4. The remaining channels also experienced high magnitude of stress range cycles during the controlled load tests with various truck positions as listed in Table 5.3.

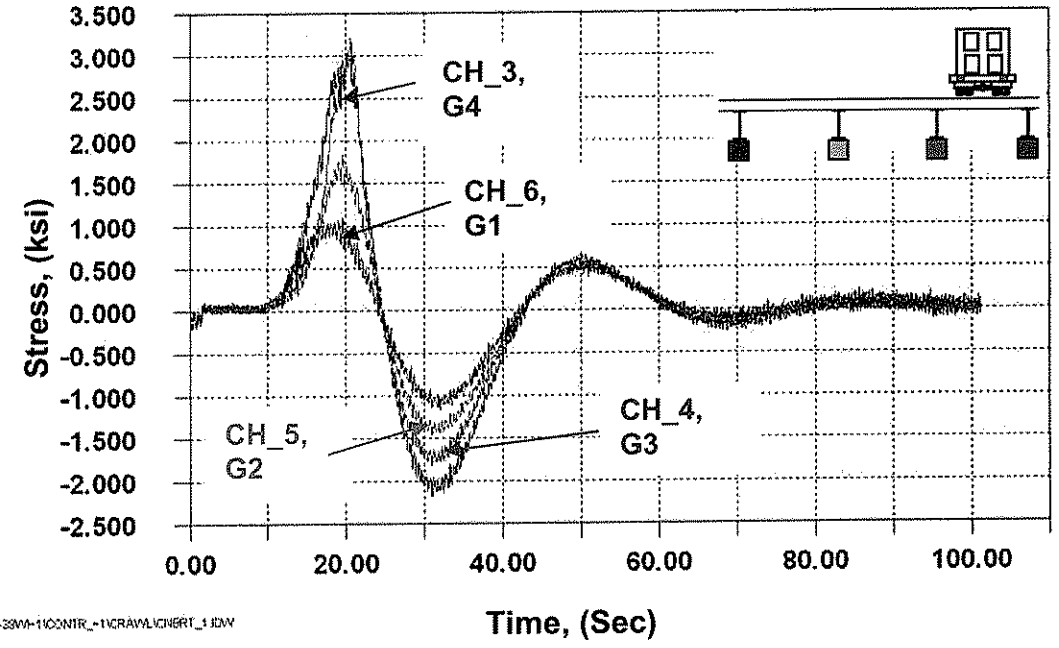

Figure 5.5 – Response of CH_3 through CH_6 installed in span 1 at P.P. 5 on girders G4 through G1 respectively (on the bottom face of the flange near welded cover plates) as test trucks # 169 passed over the right lane in the crawl test (CNBRT_1) (View looking north)

Span 1, P.P. 5						
Truck in lane	Bottom flange (ksi) (CH_3, G4)			Bottom flange (ksi) (CH_4, G3)		
	σ_{max}	σ_{min}	$\Delta\sigma$	σ_{max}	σ_{min}	$\Delta\sigma$
Right	3.0	-2.2	5.2	3.0	-1.8	4.8
Left	0.8	-1.1	1.9	1.5	-1.4	2.9
Side-by-side	3.6	-2.9	6.5	4.0	-2.9	6.9
Train (right lane)	4.3	-3.6	7.9	3.7	-3.0	6.7

Span 1, P.P. 5						
Truck in lane	Bottom flange (ksi) (CH_5, G2)			Bottom flange (ksi) (CH_6, G1)		
	σ_{max}	σ_{min}	$\Delta\sigma$	σ_{max}	σ_{min}	$\Delta\sigma$
Right	1.5	-1.4	2.9	0.9	-1.1	2.0
Left	3.0	-1.9	4.9	3.0	-2.3	5.3
Side-by-side	4.1	-3.2	7.3	4.1	-3.2	7.3
Train (right lane)	2.3	-2.4	4.7	1.4	-1.8	3.2

Span 2, P.P. 9						
Truck in lane	Bottom flange (ksi) (CH_15, G4)			Bottom flange (ksi) (CH_16, G3)		
	σ_{max}	σ_{min}	$\Delta\sigma$	σ_{max}	σ_{min}	$\Delta\sigma$
Right	2.8	-1.9	4.7	2.8	-1.5	4.3
Left	0.6	-0.8	1.4	1.3	-1.2	2.5
Side-by-side	3.7	-2.5	6.2	3.2	-2.5	5.7
Train (right lane)	3.2	-3.0	6.2	3.2	-2.4	5.6

Table 5.3 – Summary of peak measured bending stresses (ksi) in the bottom girder flanges near cover plates for various test truck lane positions in the crawl tests

5.6 Stresses in Girder Web next to Transverse Connection Plate

As previously mentioned, eight bondable strain gages were installed on the web of the main girders at the transverse connection plate detail to measure the out-of-plane bending stresses that could exist as a result of the relative displacement between the transverse connection plates and the web of the girders. The detail is classified as category C detail per AASHTO specifications with CAFL of 10 ksi.

Channels CH_7, CH_8 were installed on the web of girder G4 in span 1 at P.P. 5. Channels CH_9 and CH_10 were installed in the same span at the same panel point on girder G3. Similarly, CH_21, CH_22, CH_23, and CH_24 were installed in span 2 at P.P. 13 where CH_21 and CH_22 were installed on the web of girder G4, while CH_23 and CH_24 were installed on the web of girder G3. Figure 5.6 shows the response of CH_21 through CH_24 as the heavier test truck passed over the right lane in the crawl test CNBRT_2. All of the data are summarized in Table 5.4.

As the figure shows, the magnitude of the stress in CH_22 installed on the web of girder G4 adjacent to the transverse connection plate is considerably higher in the absolute magnitude than that of CH_24, which was installed in the same position at similar detail on girder G3. The high magnitude of stress experienced by the channel is an indication of a greater relative displacement between the transverse connection plate and the web of the girder G4. However, the magnitude of the stress range, about 5.5 ksi, is not of concern from a fatigue standpoint.

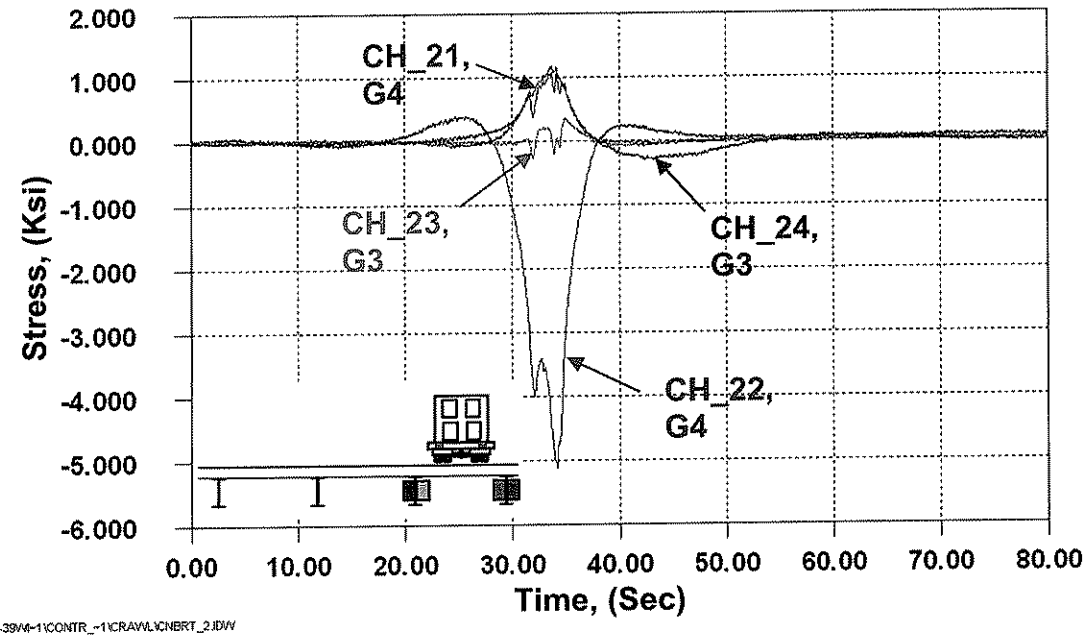

Figure 5.6 – Response of CH_21 through CH_24 installed in span 2 at P.P. 13 (on girders web adjacent to transverse stiffeners) as test truck #169 passed over the right lane in the crawl test (CNBRT_2)
(View looking north)

It is important to note that although the stress range produced by the test truck at CH_22 is not critical for fatigue, out-of-plane stresses and the potential for associated fatigue cracking can only be assessed using the random variable-amplitude data. This is because the effects of reversals and other random effects, which produce fatigue damage, are revealed during such monitoring.

Span 2, P.P. 13						
Truck in lane	Girder web (ksi) (CH_21, G4)			Girder web (ksi) (CH_22, G4)		
	σ_{max}	σ_{min}	$\Delta\sigma$	σ_{max}	σ_{min}	$\Delta\sigma$
Right	1.1	-0.1	1.2	0.4	-5.1	5.5
Left	0.1	-0.1	0.2	0.2	-0.4	0.6
Side-by-side	1.0	-0.1	1.1	0.3	-4.7	5.0
Train (right lane)	1.2	-0.1	1.3	0.4	-5.7	6.1

Span 2, P.P. 13						
Truck in lane	Girder web (ksi) (CH_23, G3)			Girder web (ksi) (CH_24, G3)		
	σ_{max}	σ_{min}	$\Delta\sigma$	σ_{max}	σ_{min}	$\Delta\sigma$
Right	0.3	-0.3	0.6	1.1	-0.3	1.4
Left	0.0	-0.2	0.2	0.2	-1.1	1.3
Side-by-side	0.3	-0.4	0.7	1.0	-0.1	1.1
Train (right lane)	0.4	-0.3	0.7	1.2	-0.5	1.7

Span 1, P.P. 5						
Truck in lane	Girder web (ksi) (CH_7, G4)			Girder web (ksi) (CH_8, G4)		
	σ_{max}	σ_{min}	$\Delta\sigma$	σ_{max}	σ_{min}	$\Delta\sigma$
Right	8.4	-0.9	9.3	0.4	-3.2	3.6
Left	0.9	-0.4	1.3	0.2	-0.3	0.5
Side-by-side	8.4	-0.6	9.0	0.3	-3.2	3.5
Train (right lane)	9.0	-0.8	9.8	0.5	-3.3	3.8

Span 1, P.P. 5						
Truck in lane	Girder web (ksi) (CH_9, G3)			Girder web (ksi) (CH_10, G3)		
	σ_{max}	σ_{min}	$\Delta\sigma$	σ_{max}	σ_{min}	$\Delta\sigma$
Right	0.1	-1.3	1.4	1.7	-0.4	2.1
Left	1.3	-0.2	1.5	0.2	-1.4	1.6
Side-by-side	0.1	-0.9	1.0	1.5	-0.2	1.7
Train (right lane)	0.1	-1.7	1.8	2.0	-0.6	2.6

Table 5.4 – Summary of peak measured bending stresses in girder webs at transverse stiffeners connections for the various test truck positions in the crawl tests

6.0 Long-term Monitoring

All twenty four strain gages and two LVDT's were chosen for long-term monitoring. The long-term monitoring of the gages was conducted from July 29, 2004 through November 3, 2004, for a total of approximately 95 days. Recording of the data in all channels was triggered when a predefined stress value was measured in CH_17 or CH_20 (CH_17 was used to trigger data recording when a heavy vehicle was passing over the right lane, while CH_20 was to trigger data recording when a heavy vehicle was passing over the left lane). For every trigger event, eight seconds of data prior to the event and eight seconds after the event were recorded. In addition to the recorded triggered events, stress-range histograms for selected channels were generated by the data logger using the rainflow cycle counting algorithm. Table 6.1 lists a summary of the channel number, the monitoring period, and whether triggered time history and stress-range histograms where developed or not.

Reference Number	Channel Number	Days Monitored (Stress-range histograms)	COMMENTS
1	CH_1	94.58	Triggered Time History / Stress-range histograms
2	CH_2	94.58	Triggered Time History / Stress-range histograms
3	CH_3	94.58	Triggered Time History / Stress-range histograms
4	CH_4	94.58	Triggered Time History / Stress-range histograms
5	CH-5	94.58	Triggered Time History / Stress-range histograms
6	CH_6	94.58	Triggered Time History / Stress-range histograms
7	CH_7	94.58	Triggered Time History / Stress-range histograms
8	CH_8	23.02	Triggered Time History / Stress-range histograms
9	CH_9	NA	NA
10	CH_10	23.02	Triggered Time History / Stress-range histograms
11	CH_11	94.58	Triggered Time History / Stress-range histograms
12	CH_12	12.11	Triggered Time History / Stress-range histograms
13	CH_13	94.58	Triggered Time History / Stress-range histograms
14	CH_14	94.58	Triggered Time History / Stress-range histograms
15	CH_15	94.58	Triggered Time History / Stress-range histograms
16	CH_16	94.58	Triggered Time History / Stress-range histograms
17	CH_17	94.58	Triggered Time History / Stress-range histograms
18	CH_18	94.58	Triggered Time History / Stress-range histograms
19	CH_19	94.58	Triggered Time History / Stress-range histograms
20	CH_20	94.58	Triggered Time History / Stress-range histograms
21	CH_21	94.58	Triggered Time History / Stress-range histograms
22	CH_22	94.58	Triggered Time History / Stress-range histograms
23	CH_23	94.58	Triggered Time History / Stress-range histograms
24	CH_24	12.11	Triggered Time History / Stress-range histograms
25	LVDT_S1	94.58	Triggered Time History
26	LVDT_S26	94.58	Triggered Time History

Table 6.1 – Summary of the channels included in the Long-term monitoring

6.1 Results of Long-term Monitoring

An estimate of the magnitude of the stresses caused by the normal daily traffic was established from the triggered time-history data as well as the stress-range histogram data collected during the monitoring period. Stresses of higher magnitude than produced by the test truck(s) were observed. Such an observation is not uncommon. As previously mentioned, the high stress-range cycles measured were a result of single and multiple vehicles crossing the bridge and were identified using the triggered data obtained from the video camera installed on the bridge.

6.1.1 Triggered Time-History Data and Video Images

As previously mentioned, high stress-range cycles measured at some of the details prompted the installation of a video camera on the bridge for accurate identification of the configuration, position, and number of trucks producing such large stress cycles. The camera was triggered by the logger when a moving vehicle caused the strain to reach a certain value in CH_17 and CH_20. Channel CH_17 and CH_20 were installed in span 2 at P.P. 13 at the welded shelf plate detail on girder G4 and G1, respectively.

The video clips collected during the monitoring period were extremely useful in determining the configuration of the vehicles causing the triggers. High stress-range cycles were recorded at some of the channels installed on the bridge and found to be caused by either a single heavy truck crossing the bridge or multiple trucks on the bridge at the same time. For example, as shown in Figure 6.1, a trigger event in CH_17 shows a measured stress-range cycle of 12 ksi. A review of the video collected during this trigger event revealed that the response was caused by mobile crane crossing the bridge in the right lane on October 20, 2004 at 5:39 pm (Figure 6.2).

In another trigger event recorded on October 21, 2004 at 7:39 am, a stress-range cycle of 9.4 ksi was measured by CH_17 (Figure 6.3). The measured stress range was caused by a flat-bed truck loaded with logs as shown in Figure 6.4.

The response of CH_17 and CH_20 to two loaded back-to-back dump trucks passing over the right lane on October 21, 2004 at 3:16 pm is shown in Figure 6.5. The time history response of the channels indicates that the response of the channels to the first truck (truck A) was slightly higher than that of the second truck (truck B). The response of CH_17 and CH_20 to the first passing truck (truck A) was approximately 9.7 ksi and 3.4 ksi and to the second passing truck (truck B) was approximately 8.4 ksi and 2.3 ksi, respectively. The slight difference in the response generated by both trucks suggests that truck B was slightly heavier than truck A. It is important to note that Figure 6.5 clearly shows separate response for each truck, suggesting that truck A had approximately passed the fifth span on the bridge when truck A was passing over the first span (Figure 6.6).

In a trigger event, which was recorded on October 28, 2004 at 7:50 am, equal response was observed by both channels (Figure 6.7) when two dump trucks were passing side-by-side (Figure 6.8). Both channels measured a stress range of approximately 10.5 ksi. The similar magnitude of response measured by both channels is an indication that both trucks were of equivalent weight and were passing over the bridge with approximately the same speed. Table 6.2 lists a summary of the above mentioned discussion and includes the stress-range cycles measured by CH_17 and/or CH_20, the type of truck, and the truck position on the bridge.

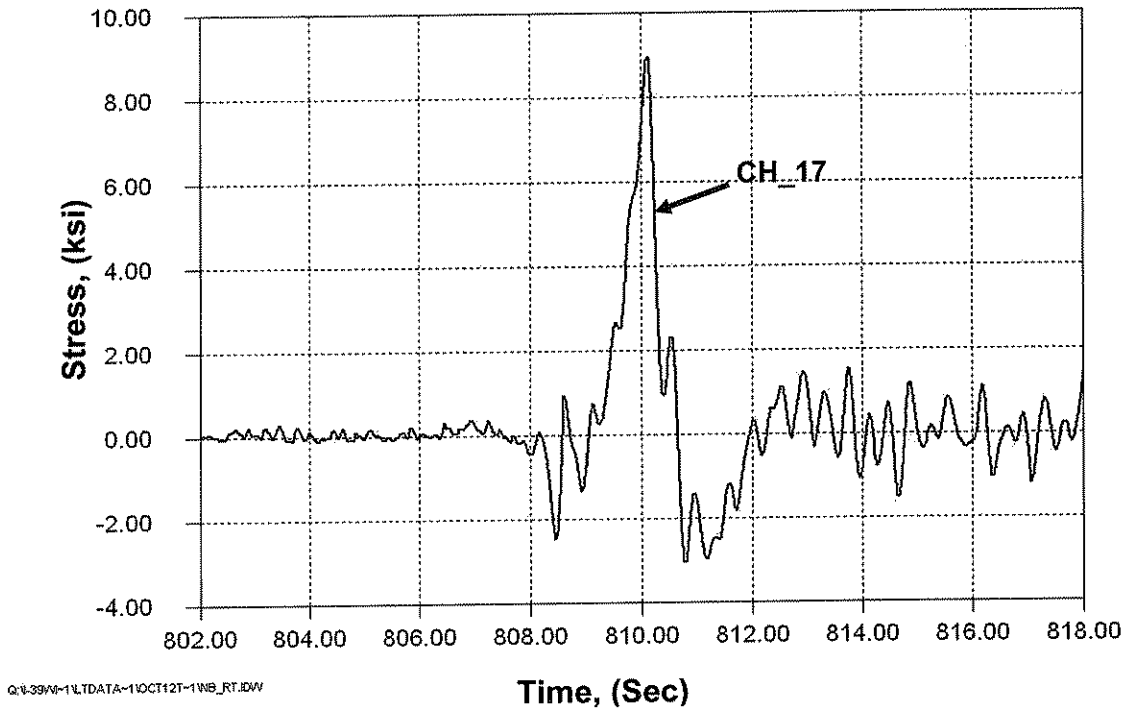

Figure 6.1 - Stress time-history for CH_17 installed in span 2 at P.P. 13 on girder G4 at welded shelf plate during the passage of a mobile crane on October 20, 2004 at 5:39 pm

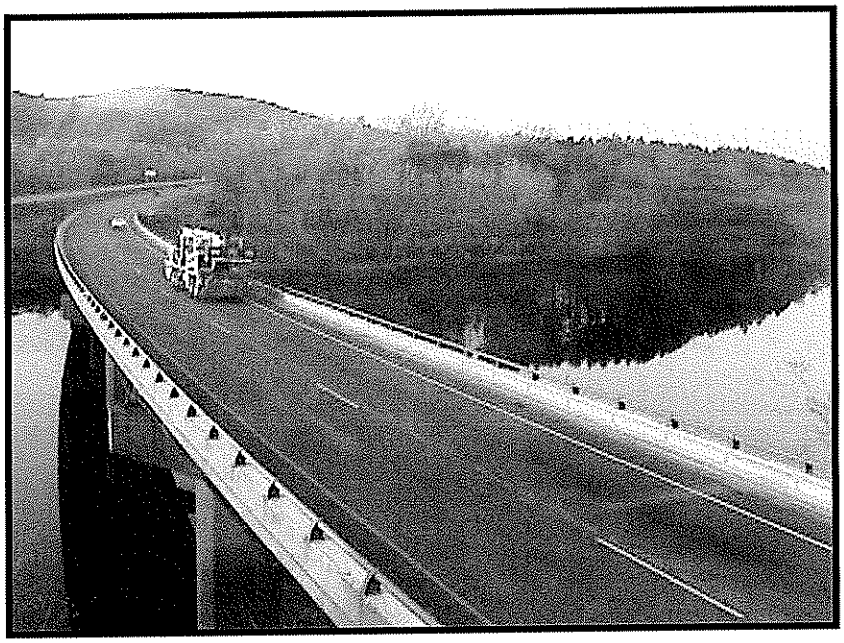

Figure 6.2 – An image from the recorded video clips during the crossing of a mobile crane on October 20, 2004 at 5:39 PM

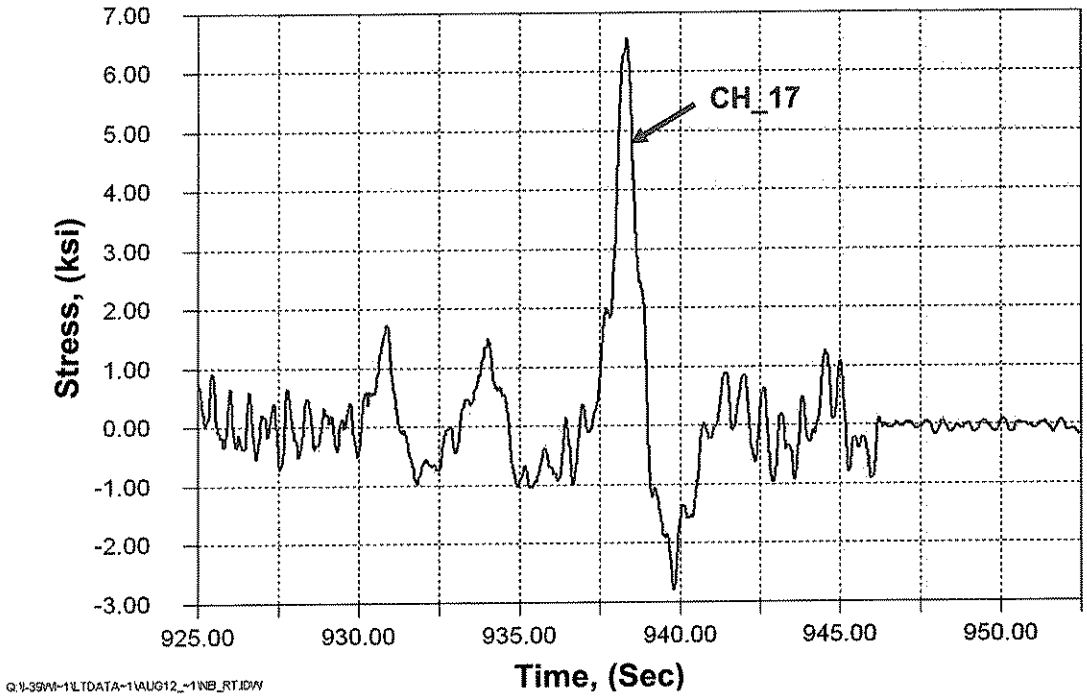

Figure 6.3 - Stress time-history for CH_17 installed in span 2 at P.P. 13 on girder G4 at a welded shelf plate detail during the passage of a flat-bed truck loaded with logs on October 21, 2004 at 7:39 AM

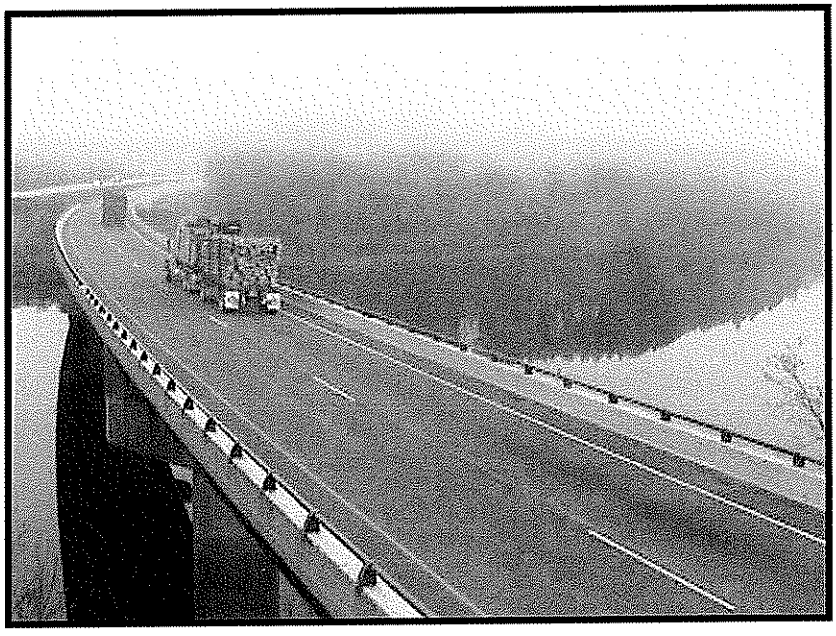

Figure 6.4 – An image from the recorded video clips during the crossing of flat-bed truck loaded with logs on October 21, 2004 at 7:39 AM

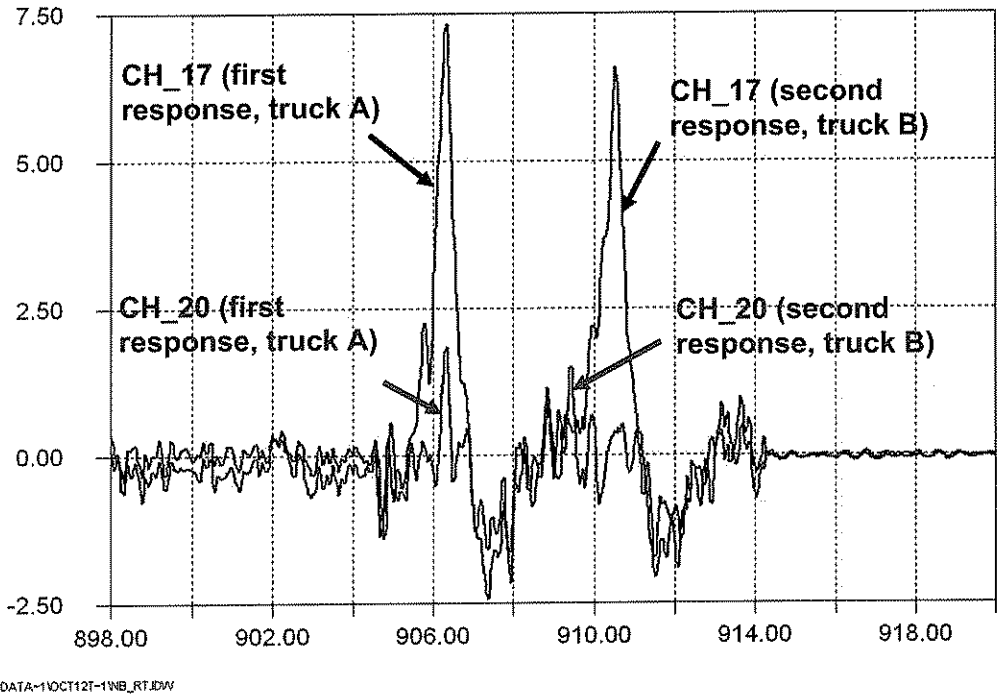

Figure 6.5 – Stress time-history for CH_17 and CH_20 installed in span 2 at P.P. 13 on girder G4 and G1, respectively at a welded shelf plate detail during the passage of two loaded dump trucks (truck "A" and truck "B") on October 21, 2004 at 3:16 PM

Figure 6.6 – An image from the recorded video clips during the crossing of two loaded dump trucks (truck "A" and truck "B") on October 21, 2004 at 3:16 PM

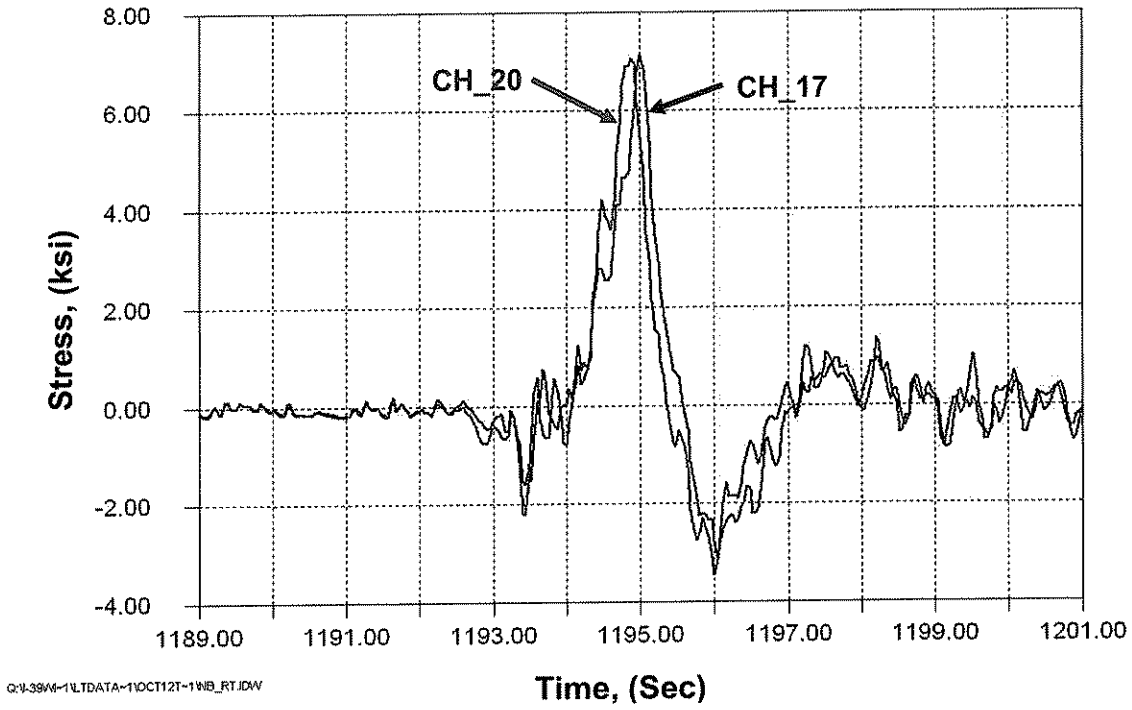

Figure 6.7 - Stress time-history for CH_17 and CH_20 installed in span 2 at P.P. 13 on girder G4 and G3, respectively at welded shelf plate during the passage of two fully loaded side-by-side dump trucks on October 28, 2004 at 7:50 AM

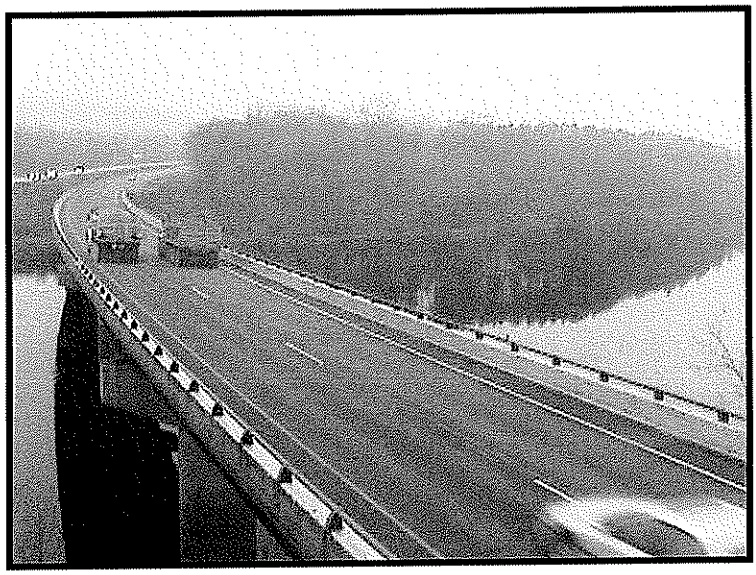

Figure 6.8 – An image from the recorded video clips during the crossing of two fully loaded side-by-side dump trucks on October 28, 2004 at 7:50 AM

Stress range	Truck Type	Truck (s) Location	Stress range
CH_17	Mobile Crane	Right lane	12 ksi
CH_17	Flat-bed	Right lane	9.4 ksi
CH_17 and CH_20	Dump Truck "A"	Right lane	9.7 ksi and 3.4 ksi, respectively
CH_17 and CH_20	Dump Truck "B"	Right lane	8.4 ksi and 2.3 ksi, respectively
CH_17 and CH_20	Dump Trucks	Side-by-side	10.5 ksi (both channels)

Table 6.2 – Summary of truck type and truck location causing a certain stress range in CH_17 and/or CH_20

6.2 Stress-Range Histograms

6.2.1 Stresses in Girder Flange at Welded Full Penetration Flange Splice

Four gages, CH_11 through CH_14, were installed on the bottom flanges of girders G1 through G4, respectively, to monitor the stresses at the welded full penetration flange splice. The detail is classified as category C per the AASHTO specifications. No stress-range cycles higher than the CAFL (10 ksi) of the detail were measured at any of the instrumented locations. The highest magnitude of stress range measured was 7.8 ksi and was recorded by CH_14, which was installed on girder G1 in span 1. Figure 6.9 shows the stress-range histogram for CH_13 and CH_14. The inset in the figure is a magnification of the right-most portion of the histogram. A lower-bound stress range truncation level of 2.5 ksi was selected for producing the histogram. Typically for fatigue evaluations, the truncation level is 1/4 to 1/3 times the CAFL of the detail. More detailed discussion on truncation levels used in fatigue evaluations could be found in Appendix B.

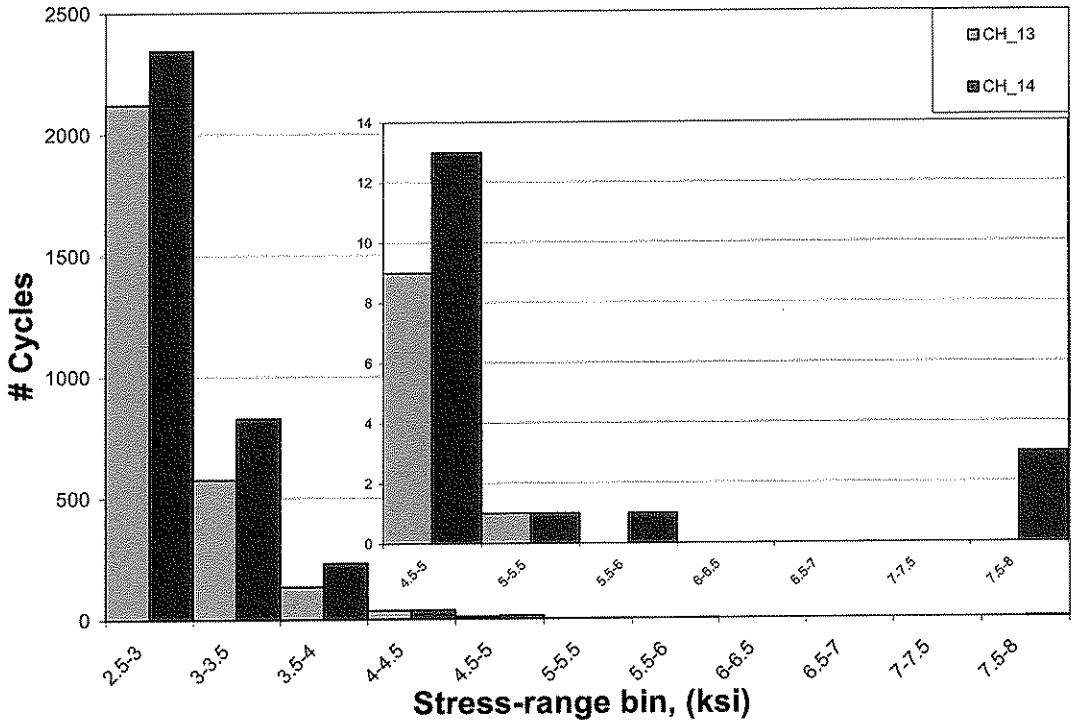

Figure 6.9 – Stress-range histogram for CH_13 and CH_14 installed at the welded full penetration flange splice

A summary of the magnitude of the maximum stress range, effective stress range, number of cycles measured per day, and the estimated remaining fatigue life for the details is presented in Table 6.3. As can be seen in the table, the fatigue life calculations indicate an infinite remaining life for all four instrumented welded full penetration flange splice details.

Channel	Fatigue Life Calculation Summary								
	S_{rmax} (ksi)	Cycles > CAFL		S_{reff} (ksi)	Cycles / Day	Days Mon.[3]	Remaining Life (Years)[2]	Cat.	Location
		#	%						
CH_11	5.75	0	0	2.9	118	94.58	Infinite	C	G4, 88'-6" from P.P. 1
CH_12	5.25	0	0	3.0	26	12.11	Infinite	C	G3, 88'-6" from P.P. 1
CH_13	5.25	0	0	3.0	30	94.58	Infinite	C	G2, 88'-6" from P.P. 1
CH_14	7.75	0	0	3.0	37	94.58	Infinite	C	G1, 88'-6" from P.P. 1

Note
1. The effective stress range and cycles per day calculations ignore cycles less than 2.5 ksi.
2. The remaining fatigue life calculations are from 2004 forward.
3. "Mon." is an abbreviation for the term monitored.

Table 6.3 - Summary of fatigue life calculations for CH_11 through CH_14 installed at the welded full penetration flange splice

6.2.2 Cover Plate at Field Splice

Six channels (CH_3 through CH_6, and CH_15 and CH_16) were installed at the termination of the cover plates used as fill plates at the flange splice details. The first four gages (CH_3 through CH_6) were installed in span 1 at P.P. 5 on girder G4 through G1, respectively. Channels CH_15 and CH_16 were installed in span 2 at P.P. 9 on girder G4 and G3, respectively.

The detail is classified as category E per the AASHTO specifications with a CAFL of 4.5 ksi. Figure 6.10 presents the stress-range histogram for CH_3 and CH_6. A lower-bound stress-range truncation level of 1 ksi (1/4 of the CAFL of the detail) was used for producing the histogram. Stress-range cycles higher than the CAFL of the detail (4.5 ksi) were recorded by both channels. The figure also shows that in the bins from 3-3.5 ksi through 5.5-6 ksi, a higher number of cycles were measured for CH_3 (right lane exterior girder) than CH_6 (left lane exterior girder). The higher count of cycles in those bins resulted in lower fatigue life estimates for CH_3 than CH_6 as shown in Table 6.4.

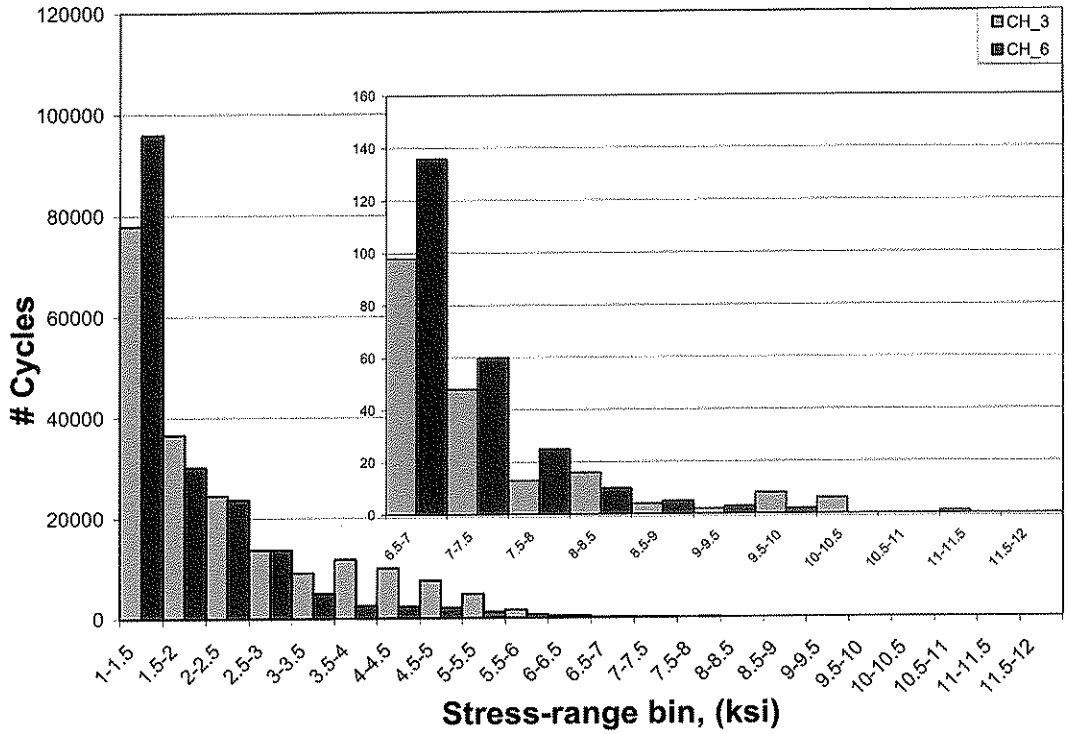

Figure 6.10 – Stress range histogram for CH_3, CH_4, CH_5, and CH_6 at the cover plate detail at flange splice

Channel	Fatigue Life Calculation Summary								
	S_{rmax} (ksi)	Cycles > CAFL		S_{reff} (ksi)	Cycles / Day	Days Mon.[3]	Remaining Life (Years)[2]	Cat.	Location
		#	%						
CH_3	11.25	14,422	7.3	2.9	2,092	94.58	19.23	E	G4, P.P. 5
CH_4	9.25	8,368	5.9	2.8	1,497	94.58	49.70	E	G3, P.P. 5
CH_5	9.25	1,981	1.4	2.4	1,521	94.58	102.14	E	G2, P.P. 5
CH_6	9.75	4,493	2.5	2.3	1,881	94.58	93.97	E	G1, P.P. 5
CH_15	8.75	4,253	3.9	2.7	1,158	94.58	95.4	E	G4, P.P. 9
CH_16	9.25	4,821	3.5	2.7	1,467	94.58	66.15	E	G3, P.P. 9

Notes
1. The effective stress range and cycles per day calculations ignore cycles less than 1.0 ksi
2. The remaining fatigue life calculations are from 2004 forward.
3. "Mon." is an abbreviation for the term monitored.

Table 6.4 - Summary fatigue life calculations of CH_3 through CH_6 and CH_15 and CH_16 installed at the cover plate field splice detail

Table 6.4 shows that the estimated remaining fatigue life of the detail is approximately between 20 and 100 years. Although in all cases positive remaining fatigue life was estimated, it is felt that improving the remaining fatigue life of the detail at locations where the estimated remaining life is below 50 years is prudent (e.g. CH_3). The suggested rehabilitation strategy is to use the hammer peening technique to improve the fatigue strength of the detail to an acceptable level. The recommended locations of the cover details to be hammer peened are further discussed in Chapter 7.

6.2.3 Lateral Shelf Plate Connection to Bottom Flange

As previously mentioned in Section 4.1.3, six channels were installed on the flanges in the longitudinal direction to measure the magnitude of the nominal stress at the lateral shelf plate detail at selected locations on the bridge. Channels CH_17 through CH_20 were installed on girder G4 through G1, respectively in span 2 at P.P. 13. The remaining two channels, CH_1 and CH_2, were installed on girder G4 and G3, respectively in span 1 at P.P. 3.

The detail where the channels were installed is classified as category detail E per AASHTO specifications and the CAFL of the detail is 4.5 ksi. Figure 6.11 presents the stress-range histogram for two of the six channels installed (CH_1 and CH_17). As shown in the figure, stress-range cycles higher than the CAFL of the detail were measured. The inset in the figure shows that stress-range cycles as high as 15 ksi were recorded by both channels during Long-term monitoring.

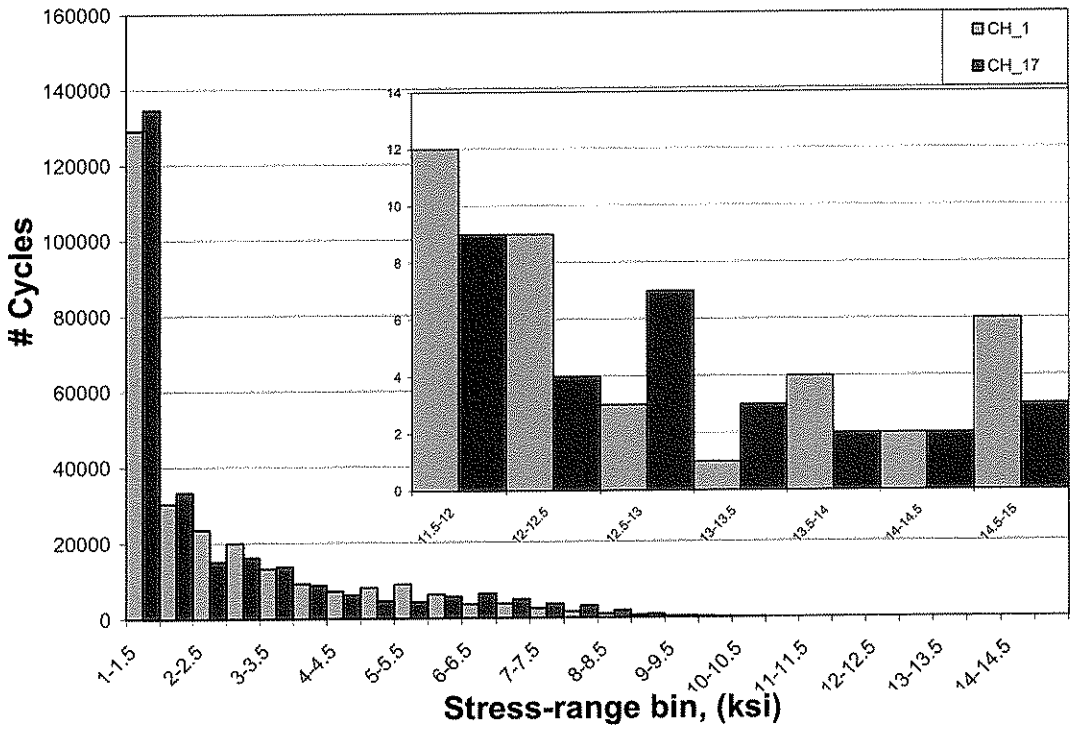

Figure 6.11 – Stress range histogram for CH_1 and CH_17

A summary of the fatigue life calculations is presented in Table 6.5. As shown in the table, the estimated fatigue life of all instrumented shelf plate details is less than 50 years. Furthermore, the calculations indicate an estimated negative remaining fatigue life at two of the instrumented locations (CH_1 and CH_17), which implies that cracking could be expected to occur at the shelf plate detail at the locations where CH_1 and CH_17 are installed. The most recent in-depth inspection of the bridge [1] indicated no sign of fatigue cracking at any of the shelf plate details on the bridge except for a 2 ¼" fabrication crack at the west shelf plate weld on edge of flange of girder G2 in span 2 at P.P. 8.

It is important to note that the number of cycles per day used in estimating the remaining fatigue life in Table 6.5 was calculated based on the rainflow data, which is assumed to be constant and well representative of the traffic volume and pattern of the bridge throughout the years for which the bridge has been in service. Clearly, this is a very conservative approach as it does not take into account that traffic volume and pattern has grown considerably since the bridge was opened to traffic. In order to address this, a modified more realistic approach was developed to account for the growth in traffic since the bridge was opened. This approach is described below.

Channel	Fatigue Life Calculation Summary								
	S_{rmax} (ksi)	Cycles > CAFL		S_{reff} (ksi)	Cycles / Day	Days Mon.[3]	Remaining Life (Years)[2]	Cat.	Location
		#	%						
CH_1	14.75	37,542	13.9	3.5	2,857	94.58	-17.97	E	G4, P.P. 3
CH_2	11.75	19,173	7.9	2.9	2,579	94.58	2.98	E	G3, P.P. 3
CH_17	14.75	36,340	13.7	3.6	2,795	94.58	-20.64	E	G4, P.P. 13
CH_18	9.75	12,462	6.4	2.9	2,076	94.58	19.05	E	G3, P.P. 13
CH_19	9.75	6,897	3.7	2.7	1,996	94.58	38.13	E	G2, P.P. 13
CH_20	12.25	8,573	3.7	2.6	2,462	94.58	29.96	E	G1, P.P. 13

Notes
1. The effective stress range and cycles per day calculations ignore cycles less than 1.0 ksi
2. The remaining fatigue life calculations are from 2004 forward.
3. "Mon." is an abbreviation for the term monitored.

Table 6.5 - Summary of fatigue life calculations of CH_1, CH_2, and CH_17 through CH_20 installed at the lateral shelf plate detail

6.2.3.1 Modified Fatigue Evaluation for Lateral Shelf Plate Connections

As stated, the estimated number of cycles per day shown in Table 6.5 was calculated based on rainflow data obtained during the period the bridge was monitored (i.e., 95 days). The calculated number of cycles per day experienced by a detail was assumed to be constant throughout the life of the bridge (i.e., same number of cycles per day for the past 43 years). Clearly, this is a conservative approach since traffic patterns and volume on the bridge has been significantly increasing over the years.

To better estimate the remaining fatigue life of the detail, actual logs of traffic data were obtained from the Wisconsin DOT [2] and used to improve the fatigue life

estimates. These traffic logs reflect the Average Daily Traffic (ADT) on the bridge for discrete years from 1964 through 2001.

However, it is not the total ADT which causes fatigue damage, but rather the Average Dailey Truck Traffic (ADTT). Vehicles weighing less than 20 kips are typically not classified as "trucks" when a fatigue evaluation is made. This assumption is commonly used as lighter vehicles have little effect on fatigue damage and is consistent with the development of the AASHTO HS-15 Fatigue Truck as described in NCHRP report 299 [3]. Thus, the ADTT must be calculated.

Because the historical data are in terms of ADT and not ADTT, the ADTT was calculated from the reported percentage of trucks which comprised the ADT data. Hence, the ADTT was estimated from the available ADT by assuming that the ADTT is approximately 12% of the ADT. This percent ADTT is reasonably conservative and is consistent with estimates of ADTT in the Wisconsin traffic data counts and previous experience. However, only discrete ADT data (and therefore ADTT data) were available from 1961 through 2001 (i.e. ADT in 1964, 1968, 1973,..., 2001).

In order to obtain ADTT data for all years, a polynomial curve was fit to the discreet ADTT data. Using the equation of the curve, ADTT values could then be calculated for any year. Once the ADTT curve was developed, the ADTT count up to the year of 2004 was then projected and calculated to be 1,855 trucks per day.

It is important to note that having ADTT data does not directly yield the cycles per day to be used in a fatigue evaluation. This is because the number of cycles per day does not necessarily equal the number of trucks which cross the bridge per day (ADTT) as individual trucks can produce multiple cycles. Furthermore, the rainflow cycle-counting method, which is used to count cycles, pairs peaks and valleys from different events to create individual cycles. Hence, it does not necessarily correspond to the number of vehicle crossing the bridge on a one-to-one basis.

To estimate the number of cycles per day at each detail from the ADTT data, a correlation was then made between the ADTT for the year of 2004 and the corresponding number of cycles/day greater than ¼ of the CAFL for the category E details of concern. This was done by taking the measured cycles/day greater than ¼ of the CAFL of the detail for a particular channel and then dividing it by the calculated ADTT. For example, using the data for channel CH_1, the number of cycles/day greater than ¼ of the CAFL was measured as 2,857 (See Table 6.5). The ADTT for 2004 was estimated to be 1,855 for this section of I-39 northbound (see Table 6.6). Hence, the relationship between the number of cycles/day and the ADTT is calculated as $\frac{2,857}{1,855} = 1.54$. This relationship (i.e. the 1.54 factor) was assumed to be constant over the life of the bridge for that particular location or channel. Hence, the number of cycles/day for that particular channel (i.e., location) would be estimated as 1.54 times the ADTT for any given year. For example, the cycles/day used for CH_1 in the year of 1964 were estimated by multiplying the adjusted ADTT for that year (see Table 6.6) by 1.54 (i.e. $333 \times 1.54 = 513\, cycles/day$).

Year	ADT NB[1]	ADTT 12% of ADT	Estimated ADTT	Estimated daily cycles[3]	Estimated yearly cycles
1964	2,165	260	333	513	187,221
1968	3,510	421	262	403	147,398
1973	2,300	276	302	465	169,778
1978	2,620	314	455	701	255,788
1984	6,040	725	744	1,145	418,026
1987	8,390	1,007	915	1,409	514,357
1991	10,920	1,310	1,156	1,781	649,968
1994	10,000	1,200	1,338	2,061	752,089
1998	12,800	1,536	1,568	2,415	881,520
2001	14,500	1,740	1,723	2,653	968,581
2004	Note 2	Note 2	1,855	2,857	1,042,805

Notes
1. Data obtained from Wisconsin DOT traffic logs
2. No traffic log data available for this year. Estimated data from curve fit
3. Cycles/day greater than ¼ CAFL of the detail

Table 6.6 - Estimated yearly cycles for discrete points representing selected years for channel CH_1

As stated, a unique ratio of the cycles/day greater than ¼ of the CAFL of the detail to the ADTT was determined for each channel. This more refined procedure was repeated for channels having lower than desired fatigue lives as estimated using the overly conservative approach discussed in Section 6.3.3.

The estimated yearly cycles were then calculated by multiplying the estimated cycles/day by 365. The total number of cycles experienced by each channel is simply obtained by adding the cycles/year for every year. Table 6.6 also shows the estimated yearly cycles for selected years. It is important to note that although traffic data were not available for some of the years between 1964 and 2004, the adjusted ADTT curve was used to estimate the ADTT corresponding to that year. The graphical representation of the process mentioned above is shown in Figure 6.12 for channel CH_1.

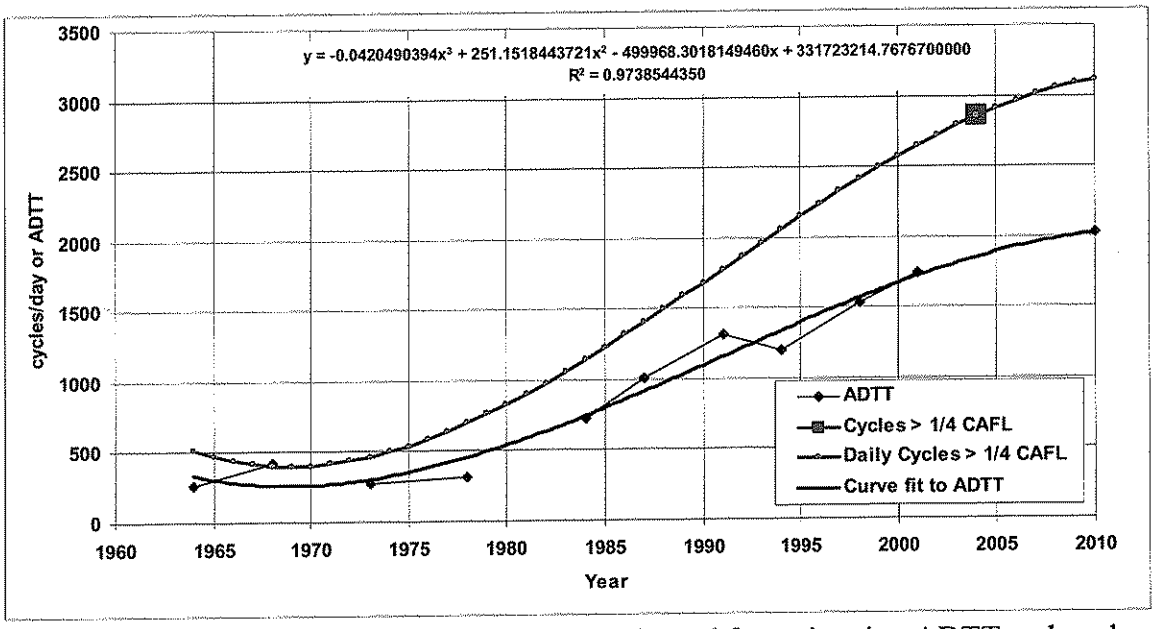

Figure 6.12 – Graphical representation of approach used for estimating ADTT and cycles for CH_1 from 1964 through 2004

As indicated in Table 6.7, the refined approach resulted in higher estimates of remaining fatigue life in CH_1 through CH_4 and CH_17 through CH_20 installed near the weld at the lateral shelf plate detail. The positive estimated fatigue life for CH_1 and CH_17 is more realistic since no cracking was observed at either of the locations where the channels were installed.

Although Table 6.7 shows positive remaining fatigue life for the channels, it is recommended that a retrofit be implemented at the lateral shelf plate connection detail where the estimated remaining fatigue life was less than 50 years (i.e. CH_1 and CH_2, and CH_17 and CH_18). Hence, all girders may not need to be retrofit at the present time. However, considering the proposed widening, it should be prudent to retrofit all girders in a given cross section. A reasonable approach would be to retrofit all shelf plates located in positive moment regions as well as those located in regions of stress reversal (e.g. P.P. 5 in span 1). Note, it is critical that these recommendations be verified

(by others) with a structural analysis model that is calibrated using measurements obtained during the controlled field monitoring of the bridge.

The suggested retrofit consists of bolting a plate to the bottom flange of the girders in the area of the shelf plates. The plate will effectively act like a bolted cover plate serving two purposes. The first is to reduce stresses in this portion of the flange. Hence, the plate must be long enough and attached with a sufficient number of bolts to ensure it is fully effective across the region where the shelf plate exists. The second advantage is that in the extremely unlikely event a fatigue crack were to form in the flange, the flange is already fully spliced thereby preventing a fracture of the girder. The dimension of the plate (i.e. thickness, width, and length) should be determined using conventional methods. The suggested retrofit scheme is illustrated in Appendix C. It is important to note that the retrofit detail shown in Appendix C will have to be modified for locations where the lateral shelf plate detail is next to cover plate field splice detail. It is also important to note that size of the plate and number of bolts shown in the sketches does not reflect the actual size to be used in the retrofit. It was only used for illustrative purpose.

Channel	Fatigue Life Calculation Summary								
	S_{rmax} (ksi)	Cycles > CAFL		S_{reff} (ksi)	Cycles / Day	Days Mon.[3]	Remaining Life (Years)[2]	Cat.	Location
		#	%						
CH_1	14.75	37,542	13.9	3.5	2,857	94.58	5.3	E	G4, P.P. 3
CH_2	11.75	19,173	7.9	2.9	2,579	94.58	26.3	E	G3, P.P. 3
CH_17	14.75	36,340	13.7	3.6	2,795	94.58	2.7	E	G4, P.P. 13
CH_18	9.75	12,462	6.4	2.9	2,076	94.58	42.4	E	G3, P.P. 13
CH_19	9.75	6,897	3.7	2.7	1,996	94.58	61.5	E	G2, P.P. 13
CH_20	12.25	8,573	3.7	2.6	2,462	94.58	53.3	E	G1, P.P. 13

Notes

4. The effective stress range and cycles per day calculations ignore cycles less than 1.0 ksi
5. The remaining fatigue life calculations are from 2004 forward.
6. "Mon." is an abbreviation for the term monitored.

Table 6.7 - Summary of the modified fatigue life calculations of CH_1 through CH_4, and CH_17 through CH_20 installed at the lateral shelf plate detail

6.2.4 Transverse Connection Plate to Web Detail

Five gages installed on the web near the web-to-flange weld to measure out-of-plane stresses in the web gap region were included in the long-term monitoring program. Specifically, CH_7, CH_8, CH_10, CH_22, and CH_24. Channel CH_7 and CH_8 were installed on the web of girder G4 at P.P. 5 in span one. CH_10 was installed in span 1 at P.P. 5 on the web of girder G3. Channels, CH_22 and CH_24 were installed in span 2 at P.P. 13 on the web of girder G4 and G3, respectively. The detail is classified as category detail C when subjected to out-plane bending since the mode of cracking originates at a weld toe. The CAFL of the detail is 10 ksi.

With exception of CH_7, no stress-range cycles higher than the CAFL were recorded at the instrumented details. However, the remaining fatigue life is estimated at being over 100 years. Infinite fatigue life was estimated for all the other locations selected for the Long-term monitoring at the transverse connection plate to web detail. At this time, there does not appear to be a need to make any retrofits at these details in the existing structural configuration. The results are summarized in Table 6.8.

Channel	Fatigue Life Calculation Summary								
	S_{rmax} (ksi)	Cycles > CAFL		S_{reff} (ksi)	Cycles / Day	Days Mon.[3]	Remaining Life (Years)[2]	Cat.	Location
		#	%						
CH_7	14.75	227	0.26	5.13	918	94.58	Over 100	C	G4, P. P. 5
CH_8	4.75	0	0.00	3.3	113	23.02	Infinite	C	G4, P. P. 5
CH_10	4.75	0	0.00	3.2	27	23.02	Infinite	C	G3, P. P. 5
CH_22	7.75	0	0.00	3.7	322	94.58	Infinite	C	G4, P. P. 13
CH_24	2.75	0	0.00	2.8	1	12.11	Infinite	C	G3, P. P. 13

Note
1. The effective stress range and cycles per day calculations ignore cycles less than 2.5 ksi.
2. The remaining fatigue life calculations are from 2004 forward.
3. "Mon." is an abbreviation for the term monitored.

Table 6.8 - Summary of fatigue life calculations of CH_7, CH_8, CH_10, CH_22, and CH_24 installed at the transverse connection plate to web detail

7.0 Summary and Conclusion

The following section provides a summary of the project and the results of the controlled load testing and long-term monitoring conducted on the I-39 Bridge in Wausau, Wisconsin.

Instrumentation Plan

1. Four fatigue prone details were instrumented to estimate remaining fatigue life. Specifically, welded full penetration flange splice details, welded cover plates at field splices, welded lateral shelf plate connections to the girder bottom flange, and out-of-plane distortion stresses at the transverse connection plate to web details.

2. Instrumentation was installed at key locations to determine the overall response of the bridge and to quantify the stress-range histograms at critical details.

Controlled Load Testing

1. The results of the controlled load tests showed good load distribution between the girders. The maximum response in the instrumented girders was observed when the test truck was directly located over the instrumented detail, as expected.

2. The response of the bridge was typical of a continuous bridge.

3. The concrete deck and girders behave compositely, as designed.

Long-Term Monitoring

1. High stress-range cycles were observed during the remote long-term monitoring program. Using a video camera, it was verified that these stresses were caused by either a single heavy truck crossing the bridge or multiple trucks on the bridge at the same time. The trucks producing the high stresses were those typically found in normal traffic spectra.

2. Stress-range histograms were developed during the long-term monitoring. The results are as follows:

    a. Infinite fatigue life was estimated for the instrumented welded full penetration flange splice details.
    b. The estimated remaining fatigue life of the cover plates at field splices is approximately between 20 and 100 years. Air-hammer peening of the weld toes is suggested to improve the fatigue strength of these details at locations where the estimated remaining life was below 50 years. The suggested locations include girder G3 and girder G4 in span 1 and span 5.
    c. Negative remaining fatigue life was estimated at the instrumented lateral shelf plate details assuming ADTT of 2004 was experienced by the detail throughout the service life of the bridge. A refined approach, which takes into account the actual traffic growth data obtained from the Wisconsin DOT since the bridge was opened to traffic, resulted in positive, more realistic estimates of the remaining fatigue life.

d. A suggested retrofit detail was developed and consisted of the addition of a plate bolted to the bottom flange of the girders. The recommended locations for the retrofit include positive moment regions as well as regions with stress reversals. The locations to be retrofit should be verified by others using a structural analysis model that is calibrated using the measurements obtained during the controlled field monitoring of the bridge.

References

1. MSA Professional Services INC., Fish Inspection and Testing, LLC., and Robert J. Connor and Associates, "B3-37-75, US 51-I 39 Northbound: Fatigue Evaluation In-depth Inspection Report", May 13, 2004.

2. Wisconsin Department of Transportation, "Wisconsin Vehicle Classification Data", Division of Transportation Investment Management, Bureau of Highway Programs, Data Management, in Cooperation with U.S. Department of Transportation, Federal Highway Administration. March, 2002.

3. F. Moses, C. G. Schilling, and K. S. Raju, "Fatigue Evaluation Procedures for Steel Bridges", NCHRP Report 299, Transportation Research Board, National Transportation Council, Washington, D.C., November 1987.

Appendix A

Instrumentation Plans

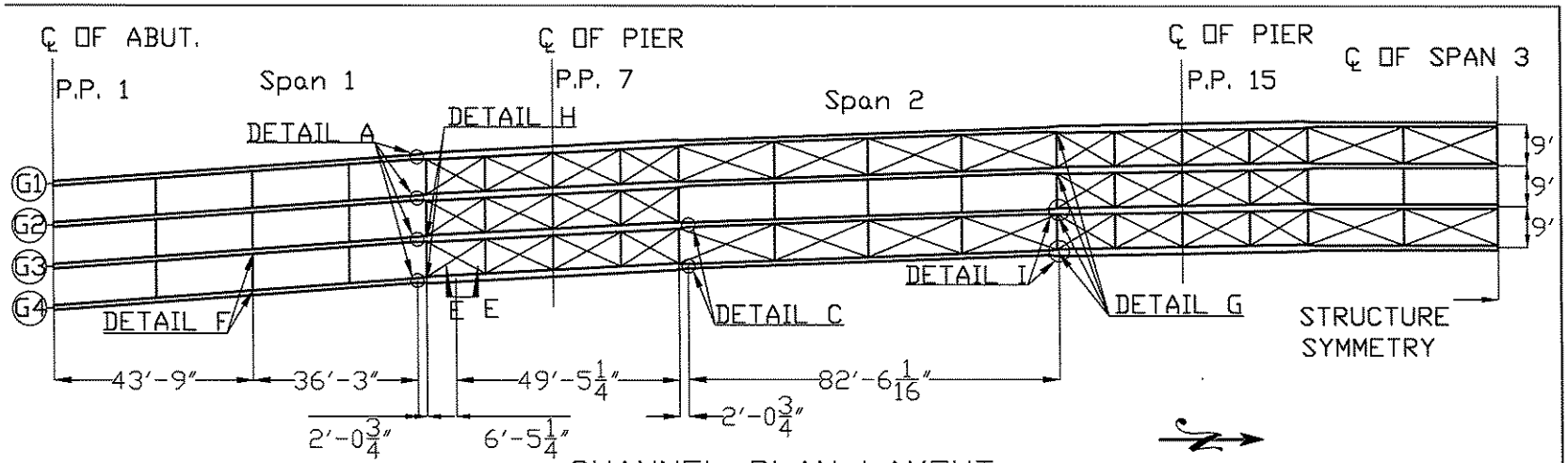

CHANNEL PLAN LAYOUT
SCALE: 1/40″=1′-0″

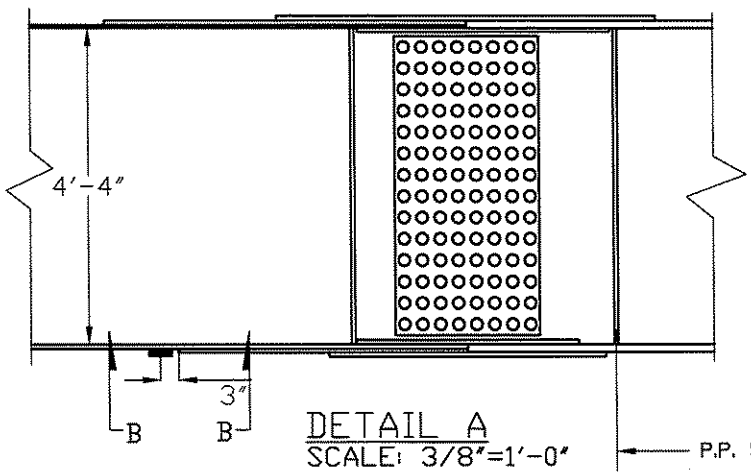

DETAIL A
SCALE: 3/8″=1′-0″

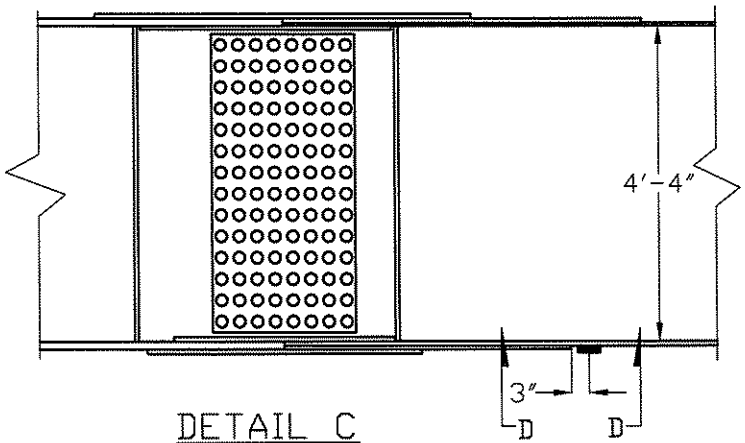

DETAIL C
SCALE: 3/8″=1′-0″

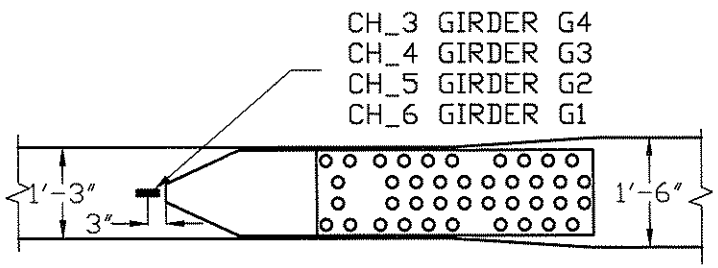

SECTION B-B: TYPICAL BOTTOM VIEW
SCALE: 3/8″=1′-0″
P.P. 5

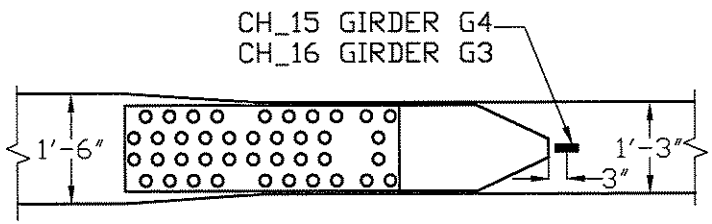

SECTION D-D: TYPICAL BOTTOM VIEW
SCALE: 3/8″=1′-0″
P.P. 9

ATLSS
ADVANCED TECHNOLOGY FOR LARGE STRUCTURAL SYSTEMS
117 ATLSS Drive
Lehigh University
Bethlehem, PA 18015
610-758-3555 FAX 610-758-6842

PROJECT:
I-39 OVER THE WISCONSIN RIVER WAUSAU, WI

SHEET NOTES:
1. ALL STRAIN GAGES ARE WELDABLE U.O.N.

NO.	DESCRIPTION	DATE	BY
1			

DESIGNED BY:	HNM
DRAWN BY:	SEM
CHECKED BY:	HNM/RJC
SCALE:	AS SHOWN
DATE:	6/30/04
PROJECT NO.:	PROJECT NO.
SHEET TITLE:	

INSTRUMENTATION PLANS

SHEET NO.:

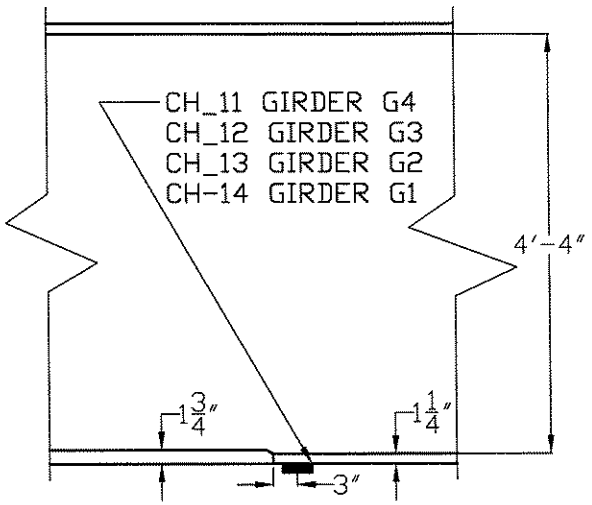

SECTION E-E: FLANGE SPLICE
SCALE: 1/2"=1'-0"
88'-6" FROM P.P. 1

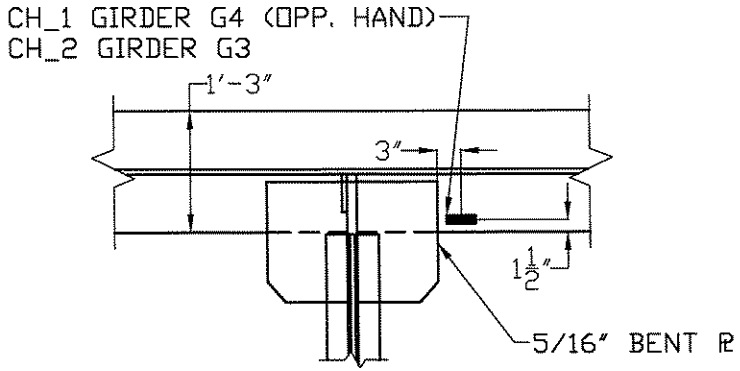

DETAIL F: LOWER SHELF PLATE AND BRACING
SCALE: 1/2"=1'-0"
P.P. 3

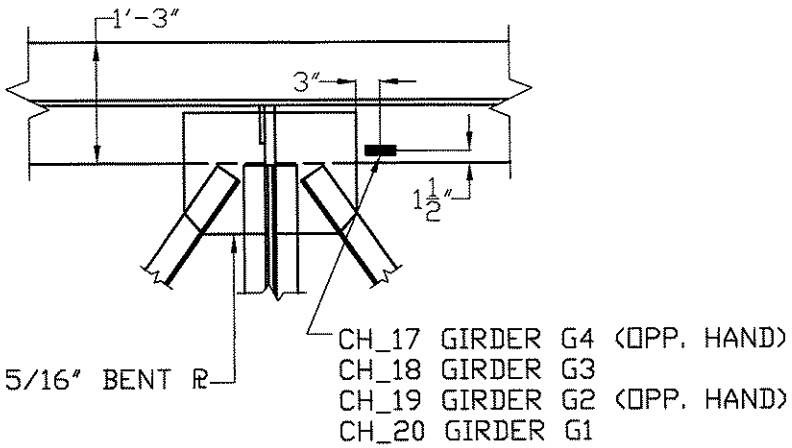

DETAIL G: LOWER SHELF PLATE AND BRACING
SCALE: 1/2"=1'-0"
P.P. 13

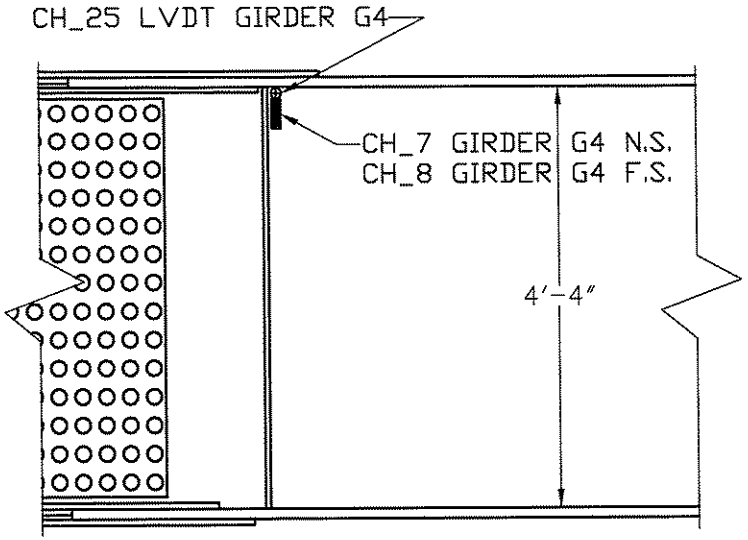

DETAIL H: BONDABLE GAGES
SCALE: 1/2"=1'-0"
P.P. 5

ATLSS
ADVANCED TECHNOLOGY FOR LARGE STRUCTURAL SYSTEMS
117 ATLSS Drive
Lehigh University
Bethlehem, PA 18015
610-758-3555 FAX 610-758-6842

PROJECT:
I-39 OVER THE WISCONSIN RIVER WAUSAU, WI

SHEET NOTES:
1. ALL STRAIN GAGES ARE WELDABLE U.O.N.

NO.	DESCRIPTION	DATE	BY
1			

DESIGNED BY:	HNM
DRAWN BY:	SEM
CHECKED BY:	HNM/RJC
SCALE:	AS SHOWN
DATE:	6/30/04
PROJECT NO.:	PROJECT NO.
SHEET TITLE:	

INSTRUMENTATION PLANS

SHEET NO.:

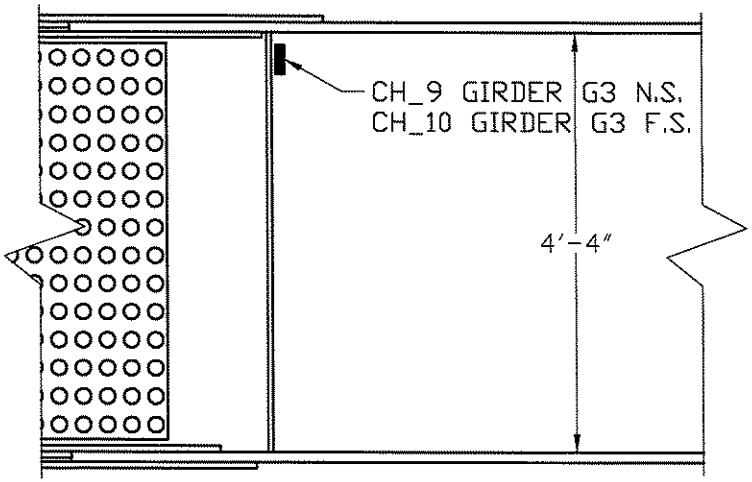

DETAIL H: BONDABLE GAGES
SCALE: 1/2"=1'-0"
P.P. 5

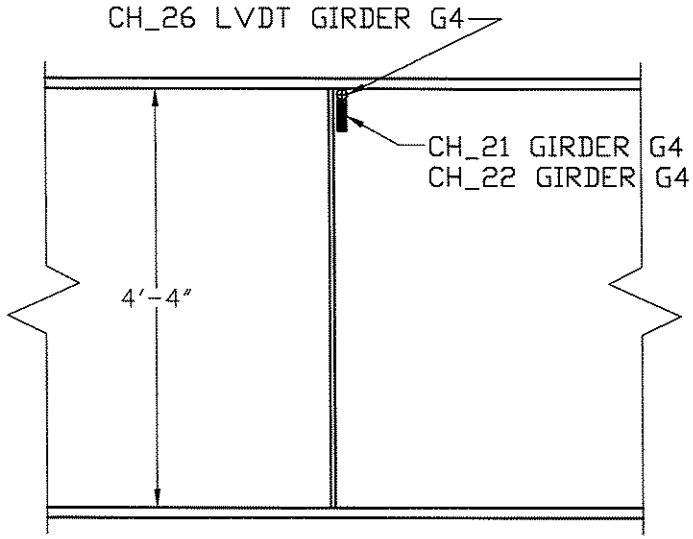

DETAIL I: BONDABLE GAGES
SCALE: 1/2"=1'-0"
P.P. 13

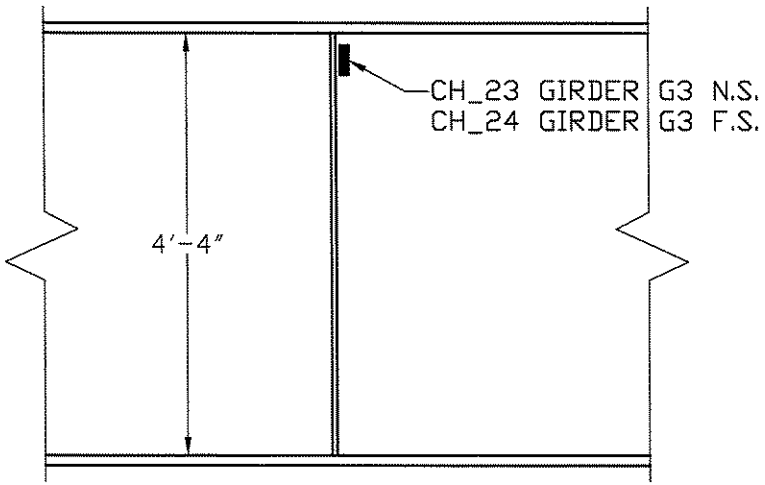

DETAIL I: BONDABLE GAGES
SCALE: 1/2"=1'-0"
P.P. 13

ATLSS
ADVANCED TECHNOLOGY FOR LARGE STRUCTURAL SYSTEMS
117 ATLSS Drive
Lehigh University
Bethlehem, PA 18015
610-758-3555 FAX 610-758-6842

PROJECT:
I-39 OVER THE WISCONSIN RIVER WAUSAU, WI

SHEET NOTES:
1. ALL STRAIN GAGES ARE WELDABLE U.O.N.

NO.	DESCRIPTION	DATE	BY
1			

DESIGNED BY:	HNM
DRAWN BY:	SEM
CHECKED BY:	HNM/RJC
SCALE:	AS SHOWN
DATE:	6/30/04
PROJECT NO.:	PROJECT NO.

SHEET TITLE:

INSTRUMENTATION PLANS

SHEET NO.:

Appendix B

Development of Stress-Range Histograms used to Calculate Fatigue Damage

Stress-Range Histograms

The stress-range histogram data collected during the uncontrolled monitoring permitted the development of a random variable-amplitude stress-range spectrum for the selected strain gages. It has been shown that a variable-amplitude stress-range spectrum can be represented by an equivalent constant-amplitude stress range equal to the cube root of the mean cube (rmc) of all stress ranges (i.e., Miner's rule) [1] (i.e., $S_{reff} = [\Sigma\alpha_i S_{ri}^3]^{1/3}$).

During the long-term monitoring program, stress-range histograms were developed using the rainflow cycle counting method [2]. Although several other methods have been developed to convert a random-amplitude stress-range response into a stress-range histogram, the rainflow cycle counting method is widely used and accepted for use in most structures. During the long-term monitoring program, the rainflow analysis algorithm was programmed to ignore any stress range less than 0.50 ksi (18με). Hence, the "raw" histograms do not include these very small cycles. Such small cycles do not contribute to the overall fatigue damage of even the worst details and if included, can actually unconservatively skew the results, as will be discussed below. It is also worth mentioning, that in some testing environments, the validity of stress-range cycles less than this are often questionable due to electromechanical noise.

The effective stress range presented for each channel in the body of the report was calculated by ignoring all stress-range cycles obtained from the stress-range histograms that were less than predetermined limits. (*It should be noted that the limit described here should not be confused with the limit described above. The limit above (i.e., 0.50 ksi (18με)) refers to the threshold of the smallest amplitude cycle that was counted by the algorithm and not related to the cycles that were counted, but later ignored, to ensure an accurate fatigue life estimate, as will be discussed.*) For all welded steel details, a cut-off or threshold is appropriate and necessary, as will be discussed. The limits were typically about ¼ the constant amplitude fatigue limit for the respective detail. For example, for strain gages installed at details that are characterized as category C, with a CAFL of 10.0 ksi, the cutoff was set at 2.5 ksi. Hence, stress range cycles less than 2.5 ksi were ignored in the preparation of the stress-range histograms used to calculate the effective stress range and the number of cycles accumulated. The threshold was selected for two reasons.

Previous research has demonstrated that stress ranges less than about ¼ the CAFL have little effect on the cumulative damage at the detail [3]. It has also been demonstrated that as the number of random variable cycles of lower stress range levels are considered, the predicted cumulative damage provided by the calculated effective stress range becomes asymptotic to the applicable S-N curve. A similar approach of truncating cycles of low stress range is accepted by researchers and specifications throughout the world [4].

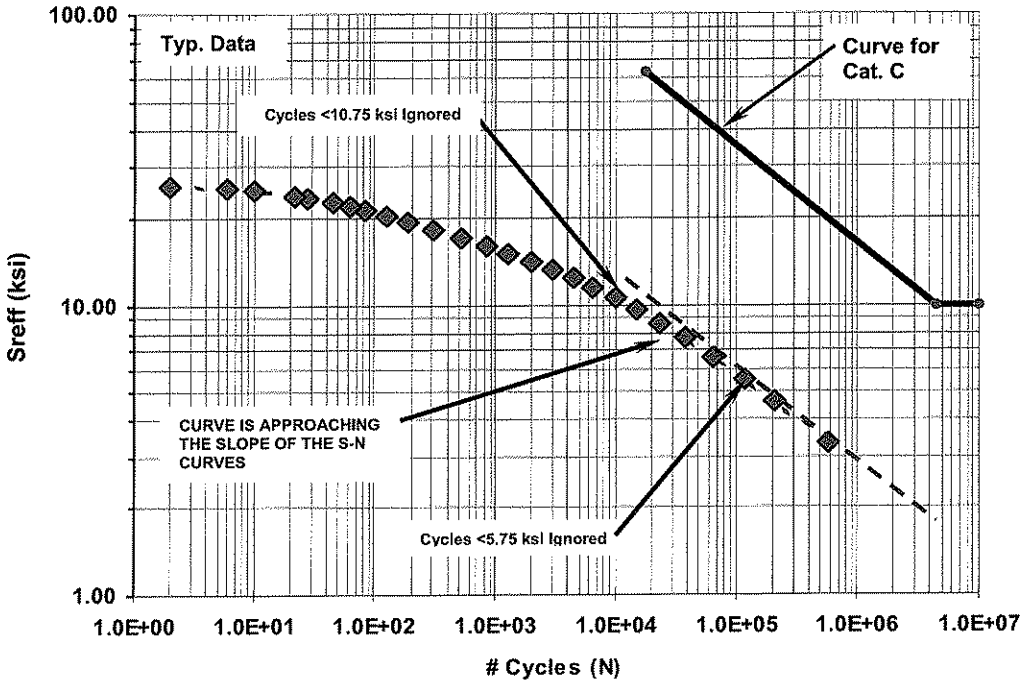

Figure B.1 – Effect of truncating cycles at different stress range cut off levels
(*Typical data from a strain gage at a fatigue sensitive detail*)

Figure B.1, shows the effect on the calculated effective stress range for several levels of truncation using typical field acquired long-term monitoring data collected from strain gage installed on a bridge. The data presented in Figure B.1 are also listed in Table B.1 showing the selected truncation level and its impact on the effective stress range.

As demonstrated by Figure B.1, as the truncation level decreases (from the lowest level), the effective stress range and corresponding number of cycles approaches the slope of the S-N curve for Category C, which is also plotted in Figure B.1 (i.e., a slope of –3 on a log-log plot). As long as the cut off level selected is consistent with the slope of the fatigue resistance curve, considering additional stress cycles at lower truncation levels does not improve the damage assessment and can therefore be ignored. As can be seen, using a truncation level as high as 10 ksi, the curve is nearly asymptotic to the slope of the S-N curves. Hence, an accurate prediction of the total fatigue life results.

It should also be noted that the load spectrum assumed in the AASHTO LRFD specifications for design was developed by only considering vehicles greater than about 20 kips [5]. Thus the AASHTO LRFD design also implicitly truncates and ignores stress cycles generated by lighter vehicles and vibration [6]. The observed frequency of stress cycles obtained from traffic counts is also consistent with the frequency of vehicles measured.

Cut Off (ksi)	Number Cycles > Cut Off Value	S_{reff} (ksi)
0.75	575,867	3.3
2.75	117,869	5.5
4.75	37,842	7.6
6.75	15,112	9.6
8.75	6,547	11.5
10.75	2,938	13.3
12.75	1,284	15.1
14.75	509	17.0
16.75	191	19.3
18.75	85	21.3
20.75	45	22.6
22.75	22	23.9
24.75	6	25.1
25.75	2	25.7

Table B.1 – Calculated effective stress ranges using different stress range cut off levels
Only every other data shown in Figure B.1 is shown for brevity

The maximum stress ranges listed in the tables developed in the body of this report were determined from the rainflow count. According to rainflow cycle counting procedures, the peak and valley that comprise the maximum stress range may not be the result of a single loading event and may in fact occur hours apart. In other words, an individual truck did not *necessarily* generate the maximum stress range shown in the tables. This is particularly true of distortion induced stresses that are subjected to reversals in stress due to eccentricity of the loading. In many cases, it was possible to identify this maximum stress range with a specific vehicle passage, but in other cases, the maximum rainflow stress range exceeded the maximum stress range from any individual vehicle. During the remote long-term monitoring program, the stress-range histograms were updated every ten minutes. Hence, the longest interval between nonconsecutive peaks and valleys is ten minutes.

References:

1. Miner, M.A., *Cumulative Damage in Fatigue*, Journal of Applied Mechanics, Vol. 1, No.1, Sept., 1945.
2. Downing S.D., Socie D.F., *Simple Rainflow Counting Algorithms*, International Journal of Fatigue, January 1982.
3. Fisher, J.W., Nussbaumer, A., Keating, P.B., and Yen, B.T., *Resistance of Welded Details Under Variable Amplitude Long-Life Fatigue Loading, NCHRP Report 354*, National Cooperative Highway Research Program, Washington, DC, 1993.
4. *Steel Structures – Material and Design*, Draft International Standard, International Organization for Standardization, 1994.
5. Schilling, C.G., *Variable Amplitude Load Fatigue, Task A - Literature Review: Volume I - Traffic Loading and Bridge Response*, Publication No. FHWA-RD-87-059, Federal Highway Administration, Washington, DC, July 1990.
6. Moses, F., Schilling, C.G., Raju, K.S., *Fatigue Evaluation Procedures for Steel Bridges, NCHRP Report 299*, National Cooperative Highway Research Program, Washington, DC, 1987.

Appendix C

Suggested Retrofit Scheme

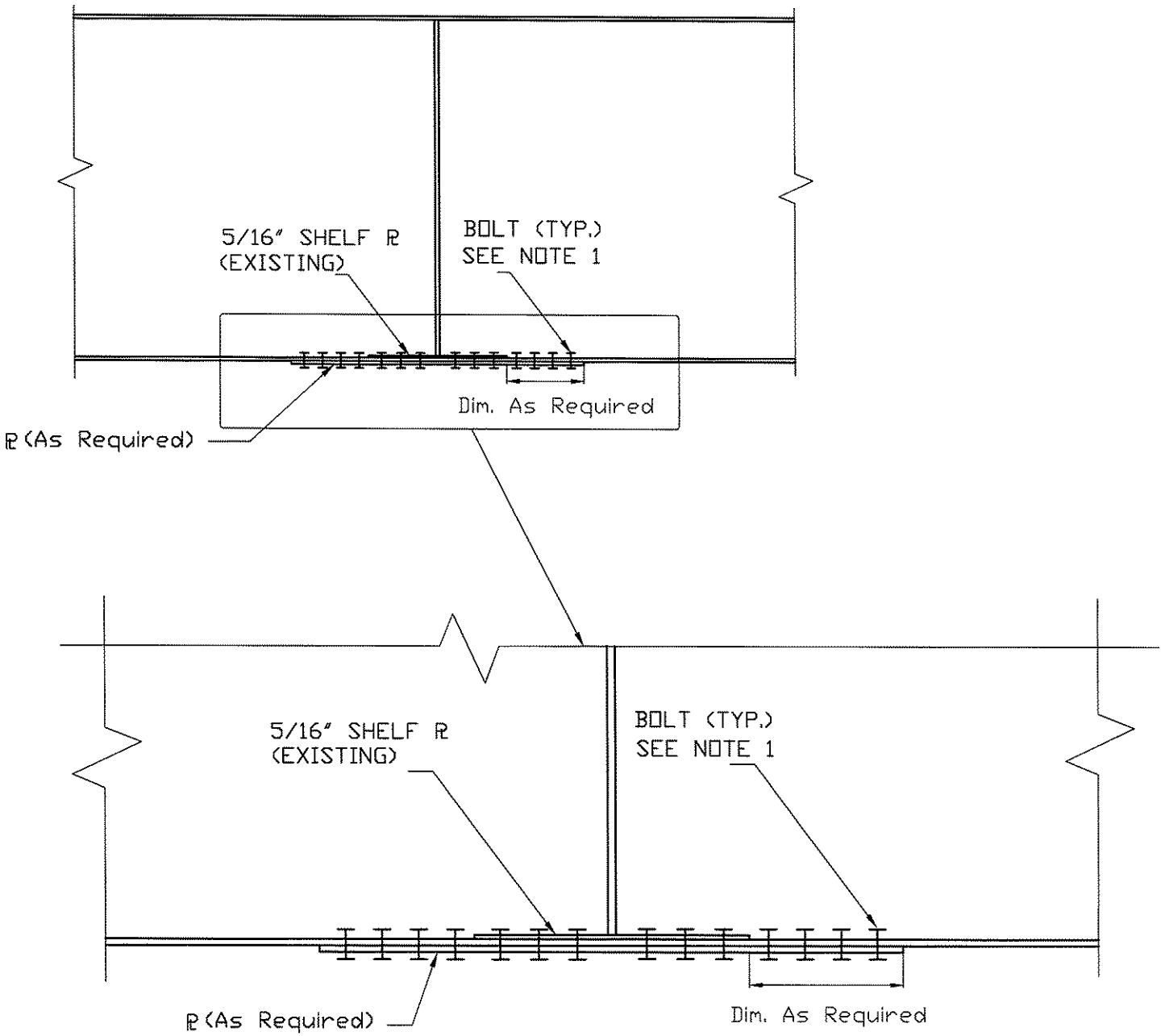

SHELF PLATE RETROFIT

ATLSS

ADVANCED TECHNOLOGY FOR
LARGE STRUCTURAL SYSTEMS
117 ATLSS Drive
Lehigh University
Bethlehem, PA 18015
610-758-3555 FAX 610-758-6842

PROJECT:

I-39 OVER THE WISCONSIN RIVER WAUSAU, WI

SHEET NOTES:

1. NUMBER AND TYPE OF BOLTS ARE AS REQUIRED

NO.	DESCRIPTION	DATE	BY
1			

DESIGNED BY:	HNM
DRAWN BY:	HNM
CHECKED BY:	RJC
SCALE:	AS SHOWN
DATE:	12/07/04
PROJECT NO.:	PROJECT NO.

SHEET TITLE:

RETROFIT PLAN

SHEET NO.: